



Calhoun: The NPS Institutional Archive
DSpace Repository

Theses and Dissertations

1. Thesis and Dissertation Collection, all items

1969

A theoretical investigation of the structure of easterly waves.

Newman, Robert L.

Monterey, California. U.S. Naval Postgraduate School

<http://hdl.handle.net/10945/13266>

Downloaded from NPS Archive: Calhoun



Calhoun is the Naval Postgraduate School's public access digital repository for research materials and institutional publications created by the NPS community. Calhoun is named for Professor of Mathematics Guy K. Calhoun, NPS's first appointed -- and published -- scholarly author.

Dudley Knox Library / Naval Postgraduate School
411 Dyer Road / 1 University Circle
Monterey, California USA 93943

<http://www.nps.edu/library>

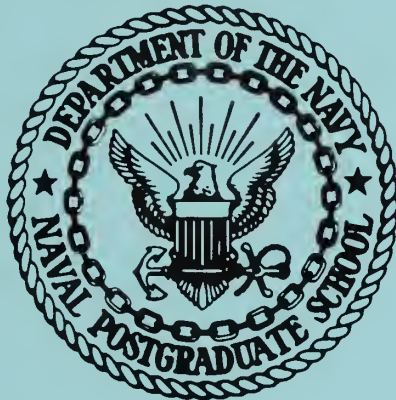
NPS ARCHIVE
1969
NEWMAN, R.

A THEORETICAL INVESTIGATION OF THE
STRUCTURE OF EASTERLY WAVES

by

Robert L. Newman

United States Naval Postgraduate School



THESIS

A THEORETICAL INVESTIGATION OF THE
STRUCTURE OF EASTERLY WAVES

by

Robert L. Newman

LIBRARY
NAVAL POSTGRADUATE SCHOOL
MONTEREY, CALIF. 93940

A THEORETICAL INVESTIGATION OF THE
STRUCTURE OF EASTERLY WAVES

by

Robert L. Newman
Commander, United States Navy
B.A., Maryville College, 1951

Submitted in partial fulfillment of the
requirements for the degree of

MASTER OF SCIENCE IN METEOROLOGY

from the

NAVAL POSTGRADUATE SCHOOL
April 1969

NPS ARCHIVE ~~Thesis N464~~ c.1
1969
NEWMAN, R.

ABSTRACT

A simple two-level numerical model using the quasi-geostrophic forecast equations is developed. Equations are linearized and friction is introduced in the surface layer. Solutions are obtained numerically by using the initial value approach. Two wind profiles, $U = -U_0 \tanh y/y_0$ and $U = U_0 \operatorname{sech}^2 y/y_0$, are used and these are known to be unstable. For each wind profile the growth rate is determined as a function of the wave number. Some observed features of easterly waves are reproduced in the numerical solutions.

TABLE OF CONTENTS

Table of Symbols and Abbreviations	5
Acknowledgments	6
SECTIONS	
1. Introduction	7
2. Basis of the Model	8
3. The Forecast Equations	9
4. Boundary Conditions and Finite Differencing Scheme . .	13
5. Wind Profiles and Initial Conditions	15
6. Computational Procedure	18
7. Results	20
8. Conclusions	38
References	40
Appendix	42
Initial Distribution List	62

TABLE OF SYMBOLS AND ABBREVIATIONS

A_e	kinematic eddy viscosity
α	inflow angle
θ_o	derivative of coriolis parameter at $y = 0$
C_p	specific heat at constant pressure
f_o	coriolis parameter at $y = 0$
g	gravity
ω	dp/dt
Ψ	gz/f_o
R	gas constant
ρ	density
\bar{T}	average temperature from some standard atmosphere
σ	$(R^2\bar{T}/p^2g) (\partial\bar{T}/\partial z + g/C_p)$
ζ	$\nabla^2\Psi$
z	height

ACKNOWLEDGMENTS

The author wishes to express his deep gratitude to Dr. Roger Terry Williams for without his patience, guidance, encouragement and counsel this thesis would have been infinitely more difficult.

A sincere thank you is also offered to Captain Thomas Kent Schminke, USAF, who cheerfully allowed his basic model to be modified for the experiments conducted.

1. INTRODUCTION

Synoptic scale disturbances in the tropical atmosphere have long been recognized (Palmer, 1951; Riehl, 1954). In general these disturbances possess a "cold-core" structure with the colder air and most active weather located east of the wave (Yanai and Nitta, 1968b). Vertical motions associated with these waves are generally upward east of the wave axis and downward to the west (Yanai and Nitta, 1967). The source of energy for these waves is not fully known, however, Charney (1963) argues that when condensation is absent the large scale motions tend to be quasi-horizontal and quasi-nondivergent. If this argument is correct then the barotropic instability that arises as the result of horizontal shear in the Intertropical Convergence Zone could be the source of energy for the disturbances (Schminke, 1968).

Kuo (1949) studied the stability characteristics of a barotropic zonal current, and showed that the barotropic zonal current is stable if the gradient of absolute vorticity has the same sign in the zonal current. Charney (1964) discussed the case where horizontal shear instability is produced in the equatorial convergence zone when the zone is located away from the equator and the converging air masses carry their angular momentum with them.

The purpose of this paper is to devise and test a numerical model that is structured realistically, that is, the perturbation has a configuration and behavior similar to observed easterly waves. The main feature desired is to have the associated weather, and therefore the vertical motion, upwind of the trough axis.

2. BASIS OF THE MODEL

The assumption that the source of energy for the wave mechanism is barotropic instability leads to the selection of a basic current that is independent of height. Baroclinicity has been omitted but the atmosphere remains stratified. Charney (1963) used a scale analysis to show that the barotropic vorticity equation governs tropical motions in the absence of condensation. In another paper Charney (1969) discusses the role of the phase velocity in energy propagation in an easterly regime. Following Schminke (1968) the assumption is made that the easterly waves can be roughly described by a two-level quasi-geostrophic model. It is recognized that the quasi-geostrophic approximation is not very accurate close to the equator, however, the zone of dynamic instability is assumed to be associated with the Intertropical Convergence Zone which is some distance from the equator so that the approximation is relatively accurate.

The type of wind profile chosen will play a large role in determining the stability of the disturbance. Jacobs and Wiin-Nielsen (1966) investigated barotropic instability and found that there are several unstable modes. Since a basic zonal current with no change in the vertical is used in this model, the wave with no vertical motion would predominate (Jacobs and Wiin-Nielsen, 1966). Easterly waves are observed to have vertical motion, so a method must be found to introduce it. This is accomplished by introducing friction in the surface boundary layer. Thus vertical motion, which depends upon the stratification of the atmosphere, is now forced into the model.

3. THE FORECAST EQUATIONS

A simple two-level model is constructed by dividing the entire atmosphere into four layers of constant pressure differential, $\Delta p/2$ (fig. 1), numbered 0 to 4 from top to bottom. Vertical motion is assumed to be zero at the

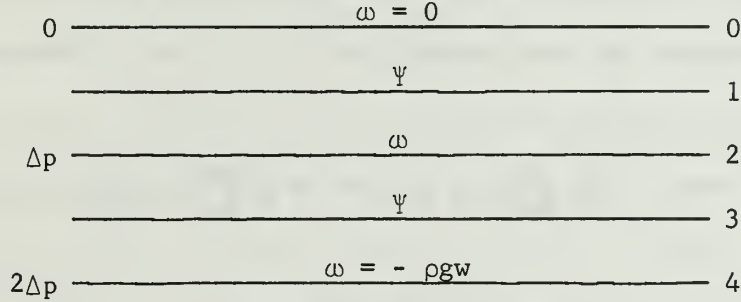


Fig. 1. Two-level model used for prediction.

top of the atmosphere, while the vertical motion term at the earth's surface is

$$\omega \approx -\rho g w_4. \quad (3.1)$$

Charney and Eliassen (1949) used the Ekman theory to derive an expression for w_4 which is

$$w_4 = \frac{1}{2} \left(\frac{2A_e}{f_o} \right)^{1/2} \sin 2\alpha \zeta_4, \quad (3.2)$$

where A_e is the kinematic eddy viscosity and α , the inflow angle. The surface geostrophic vorticity can be approximated by

$$\zeta_4 \approx \zeta_3 = \nabla^2 \psi_3. \quad (3.3)$$

Following the development of Thompson (1961), but using different notation, begin with the quasi-geostrophic vorticity equation

$$\frac{\partial}{\partial t} \nabla^2 \psi + \mathbf{k} \times \nabla \psi \cdot \nabla (\nabla^2 \psi) + \beta_o \frac{\partial \psi}{\partial x} - f_o \frac{\partial \omega}{\partial p} = 0. \quad (3.4)$$

Notice that when $\omega = 0$, the above equation becomes the barotropic vorticity equation, which is sufficient to describe the main instability.

Apply this equation at levels 1 and 3 giving

$$\frac{\partial}{\partial t} \nabla^2 \Psi_1 + |k \times \nabla \Psi_1 \cdot \nabla (\nabla^2 \Psi_1)| + \beta_o \frac{\partial \Psi_1}{\partial x} - f_o \frac{\omega_2}{\Delta p} = 0, \quad (3.5)$$

$$\frac{\partial}{\partial t} \nabla^2 \Psi_3 + |k \times \nabla \Psi_3 \cdot \nabla (\nabla^2 \Psi_3)| + \beta_o \frac{\partial \Psi_3}{\partial x} + f_o \frac{(\omega_4 - \omega_2)}{\Delta p} = 0. \quad (3.6)$$

Smaller layers could be used if it is desired to stop at some intermediate point, say the tropopause, rather than including the entire atmosphere.

Next consider the quasi-geostrophic first law of thermodynamics in the form

$$\frac{\partial}{\partial t} \frac{\partial \Psi}{\partial p} + |k \times \nabla \Psi \cdot \nabla \left(\frac{\partial \Psi}{\partial p} \right)| + \frac{\sigma}{f_o} \omega = 0, \quad (3.7)$$

where

$$\sigma = \frac{R^2 \bar{T}}{2 p g} \left[\frac{\partial \bar{T}}{\partial z} + \frac{g}{C} \right]. \quad (3.7a)$$

When this equation is applied at level 2 the result is

$$\frac{\partial}{\partial t} (\Psi_1 - \Psi_3) + |k \times \nabla \frac{(\Psi_1 + \Psi_3)}{2} \cdot \nabla (\Psi_1 - \Psi_3)| - \frac{\Delta p \omega_2}{f_o} = 0. \quad (3.8)$$

Define the following quantities

$$\Psi_m = \frac{\Psi_1 + \Psi_3}{2}, \quad (3.9)$$

$$\Psi_T = \frac{\Psi_1 - \Psi_3}{2}, \quad (3.10)$$

which implies that

$$\Psi_1 = \Psi_m + \Psi_T \quad (3.11)$$

$$\Psi_3 = \Psi_m - \Psi_T. \quad (3.12)$$

Here Ψ_T is proportional to the layer thickness, therefore is a measure of its mean temperature. Using these definitions add (3.5) and (3.6) and divide the result by 2, obtaining

$$\frac{\partial}{\partial t} \nabla^2 \Psi_m + |k \times \nabla \Psi_m \cdot \nabla (\nabla^2 \Psi_m)| + |k \times \nabla \Psi_T \cdot \nabla (\nabla^2 \Psi_T)| + \beta_o \frac{\partial \Psi_m}{\partial x} - f_o \frac{\omega_4}{2 \Delta p} = 0. \quad (3.13)$$

For the second forecast equation subtract (3.6) from (3.5) and eliminate ω_2 using (3.8)

$$\begin{aligned} \frac{\partial}{\partial t} (\nabla^2 - \mu^2) \psi_T + |k \times \nabla \psi_m \cdot \nabla (\nabla^2 - \mu^2) \psi_T + |k \times \nabla \psi_T \cdot \\ \nabla (\nabla^2 \psi_m) + \beta_o \frac{\partial \psi_T}{\partial x} + f_o \frac{\omega_4}{2\Delta p} = 0, \end{aligned} \quad (3.14)$$

where

$$\mu^2 = \frac{2f_o^2}{\Delta p^2 \sigma}. \quad (3.14a)$$

These are the prediction equations for the model. They can be linearized by separating the flow into an east-west current that varies only in y , and a small departure from this flow. In this event it is possible to treat various waves in x independently, hence the fields may be defined as follows

$$\psi_m = E(y) + A(y,t) \cos kx + B(y,t) \sin kx, \quad (3.15)$$

$$\psi_T = C(y,t) \cos kx + D(y,t) \sin kx, \quad (3.16)$$

where k is the x wave number.

Substitute expressions for ψ_m and ψ_T into (3.13) and (3.14), separate the various sine and cosine terms, neglecting all products of the quantities A through D , and equating coefficients of the cosine kx terms gives

$$\begin{aligned} \frac{\partial}{\partial t} \left(\frac{\partial^2 A}{\partial y^2} - Ak^2 \right) = k \left[\frac{\partial E}{\partial y} \frac{\partial^2 B}{\partial y^2} - \frac{\partial E}{\partial y} Bk^2 - \frac{\partial^3 E}{\partial y^3} B \right] - \\ \beta_o Bk - K \left(\frac{\partial^2}{\partial y^2} - k^2 \right) (A - C). \end{aligned} \quad (3.17)$$

For the sine terms the result is

$$\begin{aligned} \frac{\partial}{\partial t} \left(\frac{\partial^2 B}{\partial y^2} - Bk^2 \right) = k \left[\frac{\partial E}{\partial y} Ak^2 - \frac{\partial E}{\partial y} \frac{\partial^2 A}{\partial y^2} + \frac{\partial^3 E}{\partial y^3} A \right] + \\ \beta_o Ak - K \left(\frac{\partial^2}{\partial y^2} - k^2 \right) (B - D). \end{aligned} \quad (3.18)$$

Repeating the procedure for (3.16) the final equations are

$$\begin{aligned} \frac{\partial}{\partial t} \left(\frac{\partial^2 C}{\partial y^2} - Ck^2 - C\mu^2 \right) &= k \left[\frac{\partial E}{\partial y} \frac{\partial^2 D}{\partial y^2} - \frac{\partial E}{\partial y} D (k^2 + \mu^2) - \frac{\partial^3 E}{\partial y^3} D \right] \\ &- \beta_o Dk + K \left(\frac{\partial^2}{\partial y^2} - k^2 \right) (A - C), \end{aligned} \quad (3.19)$$

and

$$\begin{aligned} \frac{\partial}{\partial t} \left(\frac{\partial^2 D}{\partial y^2} - Dk^2 - D\mu^2 \right) &= k \left[\frac{\partial E}{\partial y} C (k^2 + \mu^2) - \frac{\partial E}{\partial y} \frac{\partial^2 C}{\partial y^2} + \right. \\ &\left. \frac{\partial^3 E}{\partial y^3} C \right] + \beta_o Ck + K \left(\frac{\partial^2}{\partial y^2} - k^2 \right) (B - D), \end{aligned} \quad (3.20)$$

where

$$K = \frac{f_o g}{2RT} \left(\frac{A_m}{f_o} \right)^{1/2}. \quad (3.21)$$

It is now necessary to derive the computational equation for vertical motion starting with

$$\omega_2 = \frac{2}{\Delta p \sigma} \left[\frac{\partial \psi_T}{\partial t} + u_m \frac{\partial \psi_T}{\partial x} + v_m \frac{\partial \psi_T}{\partial y} \right], \quad (3.22)$$

where

$$u_m = - \frac{1}{f_o} \frac{\partial \psi_m}{\partial y}, \quad (3.23)$$

$$v_m = \frac{1}{f_o} \frac{\partial \psi_m}{\partial x}. \quad (3.24)$$

Substituting equations (3.23), (3.24), (3.15) and (3.16) into (3.22), collecting terms, and again neglecting all products of the quantities A through D results in

$$\begin{aligned} \omega_2 &= \frac{2}{\Delta p \sigma} \left[\cos kx \left(\frac{\partial C}{\partial t} - \frac{k}{f_o} \frac{\partial E}{\partial y} D \right) + \right. \\ &\left. \sin kx \left(\frac{\partial D}{\partial t} + \frac{k}{f_o} \frac{\partial E}{\partial y} C \right) \right]. \end{aligned} \quad (3.25)$$

This is the equation used in the model for the computation of vertical motion. The prediction equations and the vertical motion equation are now in the form to be used in the model.

4. BOUNDARY CONDITIONS AND FINITE DIFFERENCING SCHEME

The finite differencing scheme used is illustrated below with a sample variable N;

$$\frac{\partial N}{\partial y} = \frac{1}{2H} (N_{i+1} - N_{i-1}) \quad (4.1)$$

$$\frac{\partial^2 N}{\partial y^2} = \frac{1}{H^2} (N_{i+1} - 2N_i + N_{i-1}) \quad (4.2)$$

$$\frac{\partial^3 N}{\partial y^3} = \frac{1}{2H^3} \left[(N_{i+2} - 2N_{i+1} + N_i) - (N_i - 2N_{i-1} + N_{i-2}) \right] \quad (4.3)$$

where i is the grid index and H is the distance between grid points.

Centered time differences are used for all quantities except those involving friction. The frictional terms are computed at time $(t - \Delta t)$. The first step in all cases is a forward time step. The second order equations for time tendencies are solved by the exact method of Richtmyer (1957, p. 101).

Yanai and Nitta (1968a) studied the problem of finite difference approximations in solving dynamic instability problems of non-divergent barotropic currents. They showed that for both symmetric and anti-symmetric zonal currents the exact boundary conditions can be replaced by rigid boundary conditions at a distance equal to the half width of the shearing wind belt. At any boundary distance larger than this value the numerical and theoretical values tended to have a constant difference. Therefore rigid boundaries are placed at $y = -w/2$ and $y = w/2$, where w is the total width over which computations are made. With the exception of E (the basic current) all variables have the boundary condition $A = B = C = D = 0$ at $y = -w/2$ and at $y = w/2$. When second derivatives are required on the boundary they are set equal to zero.

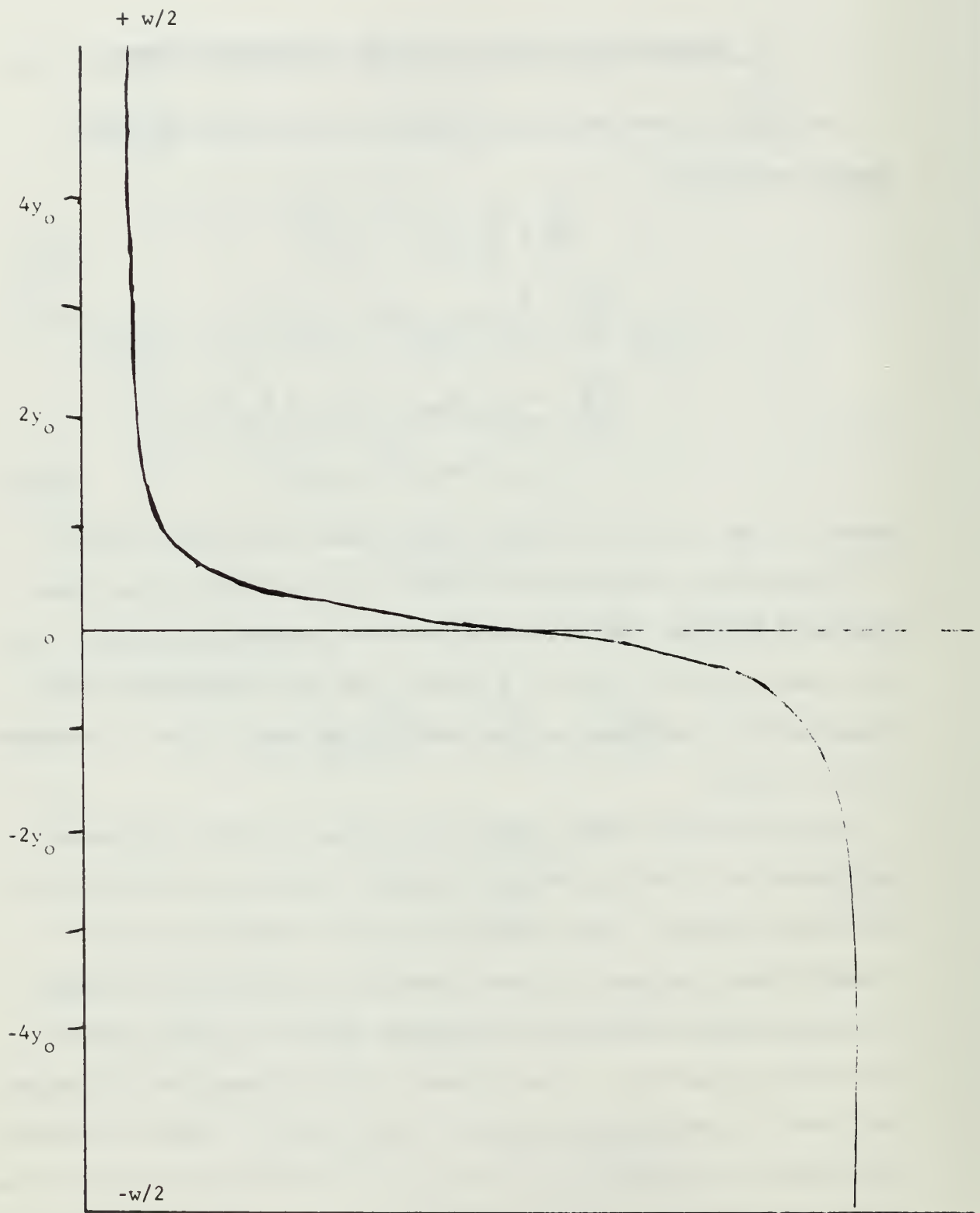


Fig. 2. Wind profile $U = -U_0 \tanh y/y_0$.

5. WIND PROFILES AND INITIAL CONDITIONS

Schminke (1968) investigated and discussed the structure of easterly waves from a similar model using one wind profile ($U = -U_0 \tanh(y/y_0)$) and one non-dimensional wave number ($1/2y_0$). It is proposed to expand this to include another profile ($U = U_0 \operatorname{sech}^2 y/y_0$). Additionally the behavior of disturbances at various non-dimensional wave numbers under both profiles will be considered.

Charney (1963) shows by scale analysis that in the absence of condensation, flow in the tropics is governed by the barotropic vorticity equation. The assumption is made that the source of energy for easterly waves must be barotropic instability. Since potential energy is assumed not to be an important energy source the basic temperature field may be set equal to a constant and is invariant. However, small temperature fluctuations are observed with easterly waves, so a two level model is needed (Schminke, 1968).

If the waves are to grow, the zonal wind profile must be barotropically unstable. Following the suggestion of Charney (1963) that the shear layer near the Intertropical Convergence Zone may be formed by transport of angular momentum, the unstable profile chosen to approximate this is

$$U = -U_0 \tanh y/y_0, \quad (5.1)$$

illustrated in figure 2. This seems most appropriate during monsoonal conditions. The second profile chosen,

$$U = U_0 \operatorname{sech}^2 y/y_0, \quad (5.2)$$

is probably more applicable to mean flow conditions, and is illustrated in figure 3.

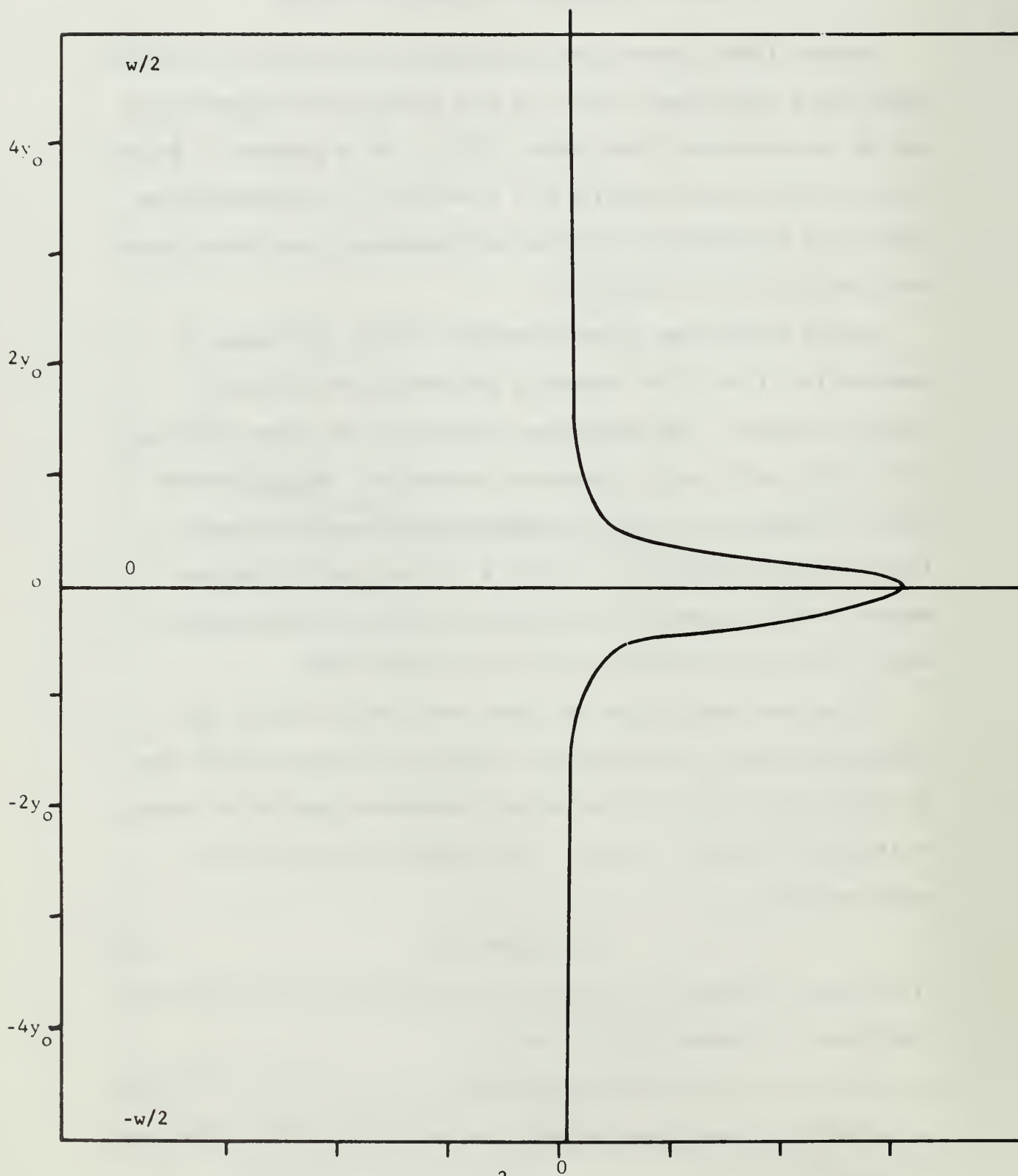


Fig. 3. Wind profile $U = U_0 \operatorname{sech}^2 y/y_0$

Garcia (1956) found that the profile given in (5.1) is barotropically unstable when $0 \leq k \leq y_0^{-1}$. Betchov and Criminale (1967) have analytically, and by use of the eigenvalue approach, investigated this profile throughout the range mentioned above and found the maximum instability at a non-dimensional wave number of 0.45 ($ky_0 = 0.45$). With these results in mind this paper is confined to the range 0.25 to 0.60 for the non-dimensional wave number when dealing with the hyperbolic tangent profile (5.1). Betchov and Criminale (1967) found a rather flat zone of maximum instability for the hyperbolic secant squared profile (5.2) in the range 0.80 to 1.05 for the non-dimensional wave number. Some computations were done in the lower range (0.25 to 0.60), but the majority of the experiments with this profile were confined to the range 0.70 to 1.15. Results of experiments with both profiles will be discussed in a later section.

With the wind profile independent of height and with no friction Ψ_m and Ψ_T should behave independently. Jacobs and Wiin-Nielsen (1966) showed that the growth rate for the Ψ_m field is greater than that for the Ψ_T field. The thermal field Ψ_T is zero in the initial state but it changes as a result of the Ekman friction term. Ψ_m is introduced into the model as a random disturbance in y . Introduction of surface friction leads to the coupling of the two fields. Thus at time $t = 0$

$$A = \text{random disturbance } (y), \quad (5.3)$$

$$B = \text{random disturbance } (y), \quad (5.4)$$

$$C = 0 \quad (5.5)$$

$$D = 0 \quad (5.6)$$

$$E = U_0 y_0 \ln(\cosh(y/y_0)), \quad (5.7)$$

or
$$E = U_0 y_0 \tanh y/y_0. \quad (5.8)$$

6. COMPUTATIONAL PROCEDURE

A list of the constants used in the computations is given below;

$$y_o = 200 \text{ kilometers,}$$

$$w = 2000 \text{ or } 4000 \text{ kilometers,}$$

$$U_o = 10 \text{ meters per second,}$$

$$f_o = 5 \times 10^{-5} \text{ per second,}$$

$$\sigma = 0.8 \text{ meters per second squared per centibar squared,}$$

$$\beta = 0.0 \text{ or } 2.29 \times 10^{-11} \text{ per meter per second,}$$

$$\Delta p = 50 \text{ centibars,}$$

$$A_e = 10 \text{ meters per second squared,}$$

$$\alpha = 22.5 \text{ degrees,}$$

$$\mu^2 = 2.49 \times 10^{-12} \text{ per meter squared,}$$

$$H = 25 \text{ or } 50 \text{ kilometers,}$$

$$\Delta t = 0.5 \text{ or } 1.0 \text{ hours.}$$

When $w = 2000$ km and $H = 50$ km a forecast period of 14 days was used, in all other cases the forecast period was 28 days. A sample program as developed by Schminke (1968) and modified to fit the IBM 360 computer is included as Appendix 1 (note: this program is for $w = 2000$ km and $H = 25$ km).

The random disturbance introduced into the Ψ_m field, (5.3) and (5.4), was generated by a random number generation program, then read directly into the computer. The same disturbance field was used for all experiments with both variations of β , H , Δt , and all variations of the non-dimensional wave number. After a few days the disturbance adjusted to an exponential growth. For convenience, growth rates were computed over the last three days of the forecast period. Once the field has adjusted it does not matter when computed, rates are always

the same. This was done by assuming the amplitudes could be written as

$$x_1 = S \exp (U_o n / y_o) t_1, \quad (6.1)$$

$$x_2 = S \exp (U_o n / y_o) t_2, \quad (6.2)$$

where n is the growth rate and S is a constant. By forming the ratio x_2/x_1 , the growth rate can be shown to be

$$n = \frac{y_o \ln (x_2/x_1)}{U_o (t_2 - t_1)} . \quad (6.3)$$

7. RESULTS

A series of experiments was conducted under varied conditions. In general the total distance over the grid was 2000 km, but one series was done over a total distance of 4000 km. Grid mesh was either 50 km or 25 km with the smaller distance producing better results. When the grid mesh was 25 km a time step of 0.5 hours was used, however the majority of experiments were run at $t = 1.0$ hours. All cases were run with $\beta = 0$, then with $\beta = 2.29 \times 10^{-11}$ meters per second. Many combinations of friction, wave number and wind profile were run, and selected ones are illustrated in figures 4 through 19.

Growth rates for the disturbances with both profiles and for various non-dimensional wave numbers are shown in figures 4 through 11. Betchov and Criminale (1967) found a maximum growth rate of approximately 0.19 for a non-dimensional wave number of 0.45 using the hyperbolic tangent profile. With rigid boundaries, no friction and a fairly large grid size ($H = 25$ km) through the maximum shear zone (width approximately 400 km), the result (fig. 7) was a growth rate of 0.165 at a wave number of 0.45. According to Yanai and Nitta (1968a) the best results should be obtained with a minimum of 20 grid steps across the zone of maximum shear. Therefore the results for the hyperbolic tangent profile are considered good, and the trend upward toward the Betchov and Criminale (1967) results is evident as the grid size is decreased (compare figures 5 and 7). The inclusion of the β parameter had no significant effect on the growth rates giving only a slight decrease of 0.01 or less.

The hyperbolic secant squared profile results were equally encouraging. Just as Betchov and Criminale (1967) lead one to expect, a relatively broad zone of maximum growth is found reaching from 0.85 to 0.95 non-dimensional wave numbers. It is difficult to ascertain just what maximum rate Betchov and Criminale (1967) found, however, results of these experiments show rates that are significantly smaller than the rates for the hyperbolic tangent profile. The inevitable conclusion is that the hyperbolic secant squared profile is not quite as unstable as the hyperbolic tangent profile. As before, decreasing the grid size in the maximum shear area led to larger growth rates. Figures 9 and 10 illustrate this very well.

In figures 12 through 15 the amplitude and phase relationships of Ψ_m , Ψ_T and ω are depicted for the wave number of maximum growth. Amplitudes of Ψ_m , Ψ_T and ω show maxima in the region of greatest horizontal shear. The influence of the frictional term is clearly seen in the relative amplitudes of Ψ_1 and Ψ_3 . The three fields show close phase relationships and all phases change rapidly through the shear zone. It appears to be a safe assumption that the temperature and pressure fields are in close relation for both levels. The omega amplitude (fig. 14) shows a distinct minimum in the center of the field but sharp maximum peaks on each side in the maximum shear zone. Phase relations between Ψ_3 and ω might almost be termed ideal with the sinking motion north of the shear zone about 70 degrees upwind of the amplitude ridge, placing the convergence in the area where it is normally observed in easterly waves.

Addition of the β parameter made small insignificant changes in the amplitude; phase relationships maintained the same basic pattern as

without β . Variation in the non-dimensional wave number over the range 0.25 to 0.60 left the pattern basically unchanged while producing the growth rate changes discussed above.

Figures 16 through 19 illustrate the behavior of the hyperbolic secant squared profile. Note that Ψ_1 far exceeds the other components in amplitude (fig. 16) and that the maximum is symmetrical around the center of the maximum shear zone. Ψ_3 is very small indicating that friction is probably more effective with the hyperbolic secant squared profile. The lower field, Ψ_3 , tends to lead the upper field in westward movement. This appears reasonable and is observed in tropical disturbances of this nature (Riehl, 1954, pp. 215). This gives the entire system a tilt toward the east with increasing height; this tilt is not noticeable with the hyperbolic tangent profile.

The omega amplitude is very sharp peaked and symmetric about the center. Velocities, from about $\pm y_0$ to the boundaries, are very small. In this area the convergence appears to be about 100 degrees out of phase with the trough. Near $y_0 = 0$, along the Intertropical Convergence Zone, the convergence actually leads the trough.

Use of a finite value for the β parameter made no significant difference in the results with this profile.

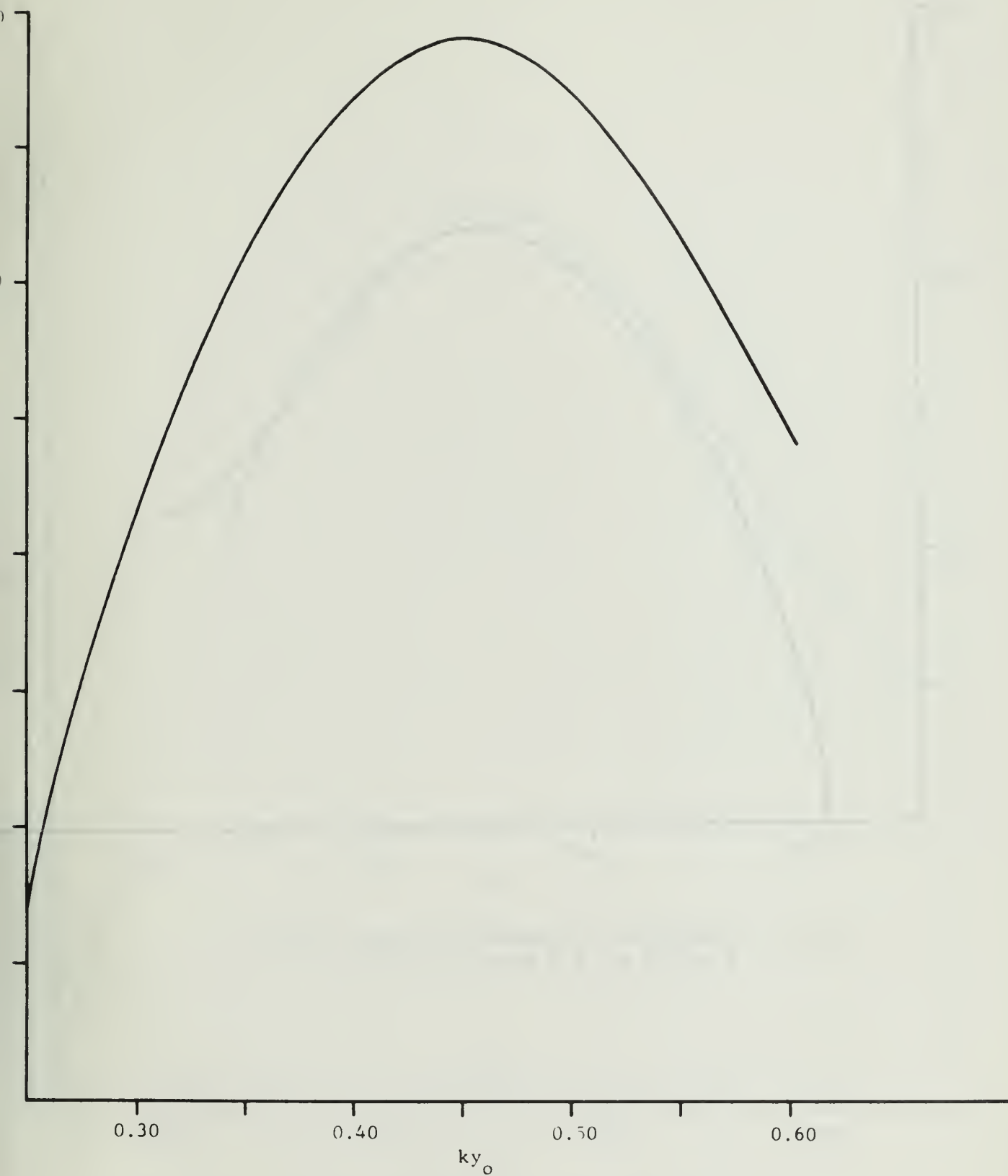


Fig. 4. Growth rate for hyperbolic tangent profile,
 $w = 2000$ km, $H = 50$ km, with friction.

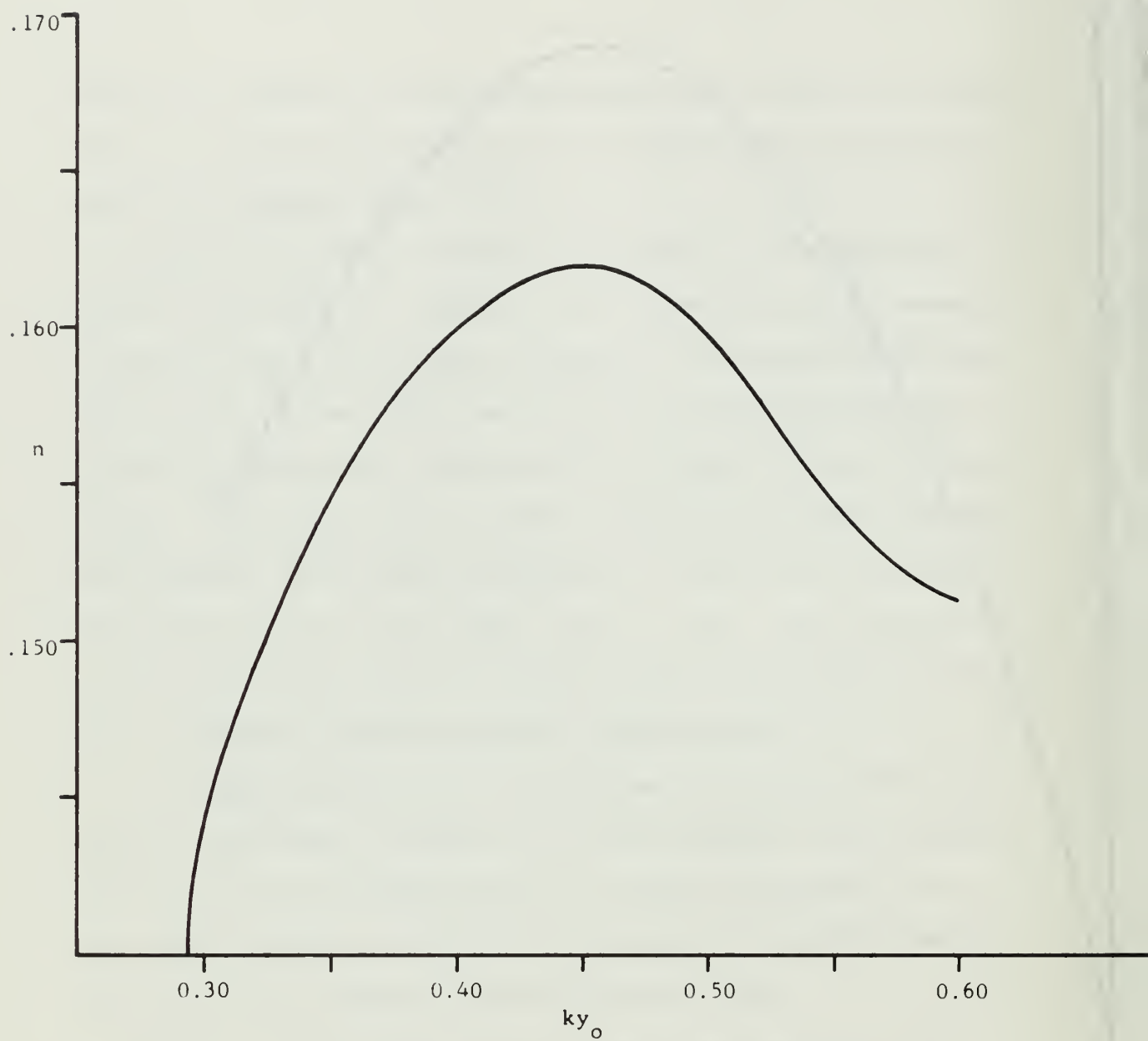


Fig. 5. Growth rate for hyperbolic tangent profile,
 $w = 2000$ km, $H = 50$ km, no friction.

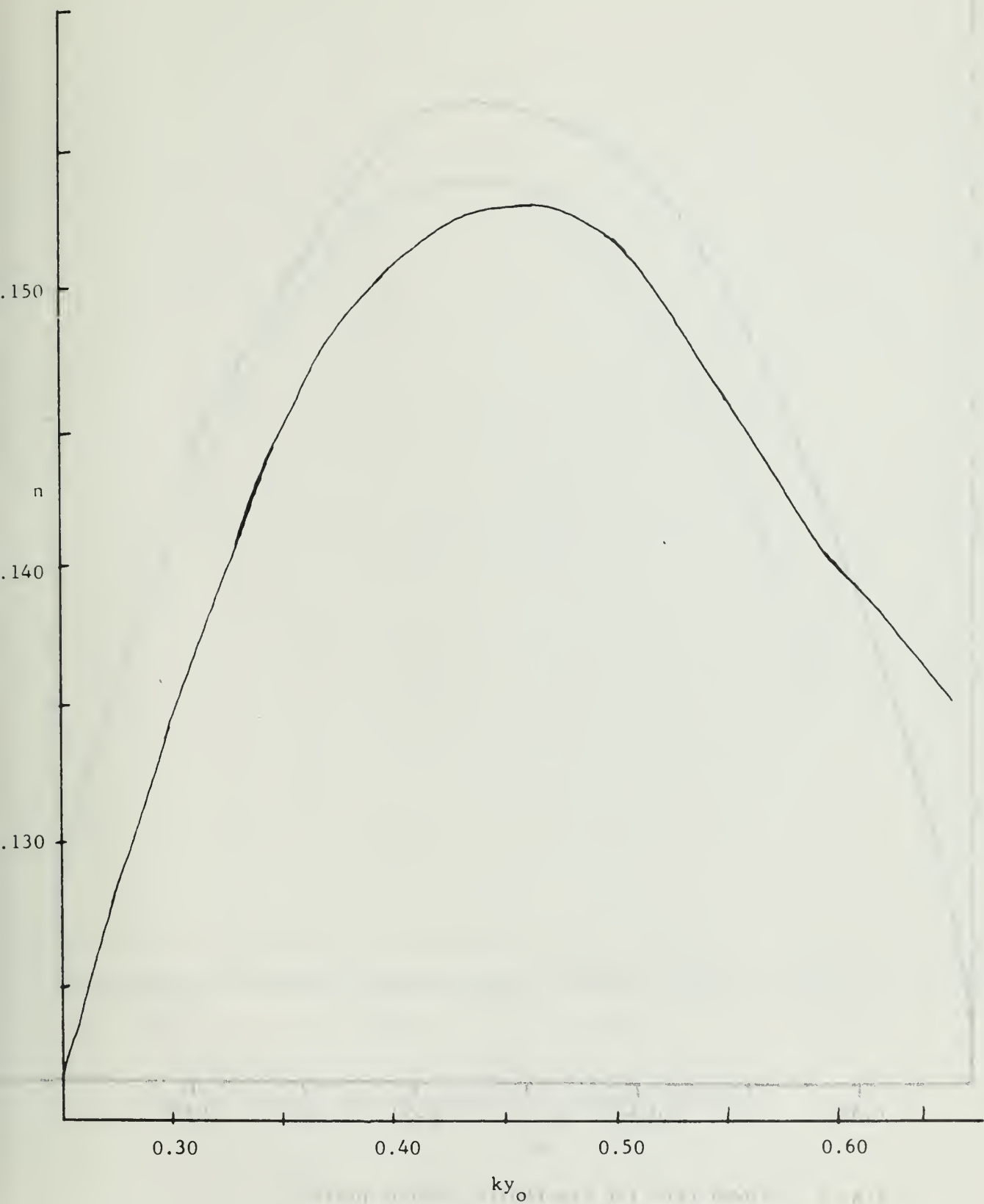


Fig. 6. Growth rate for hyperbolic tangent profile,
 $w = 2000$ km, $H = 25$ km, with friction

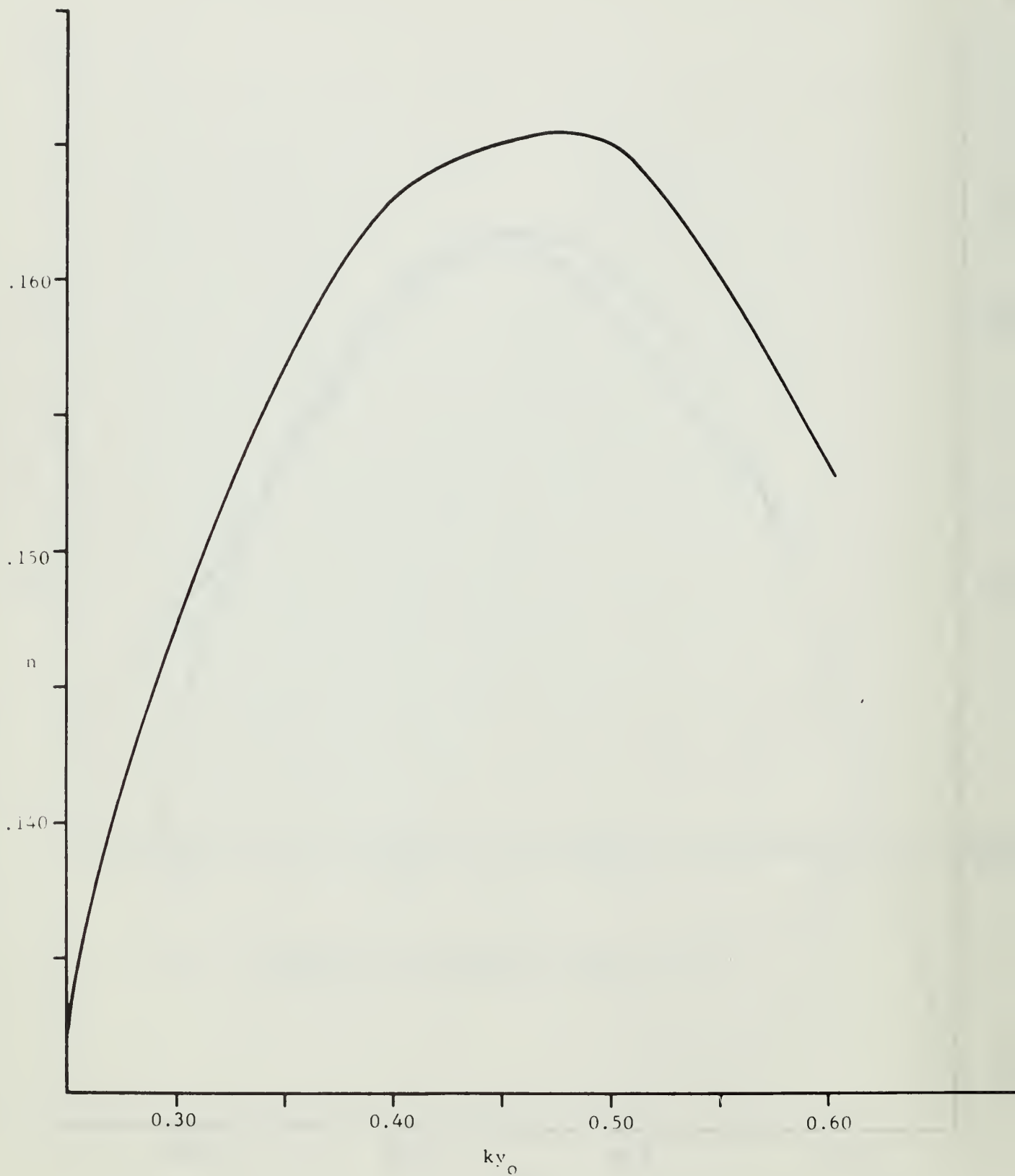


Fig. 7. Growth rate for hyperbolic tangent profile, $w = 2000$ km, $H = 25$ km, with no friction.

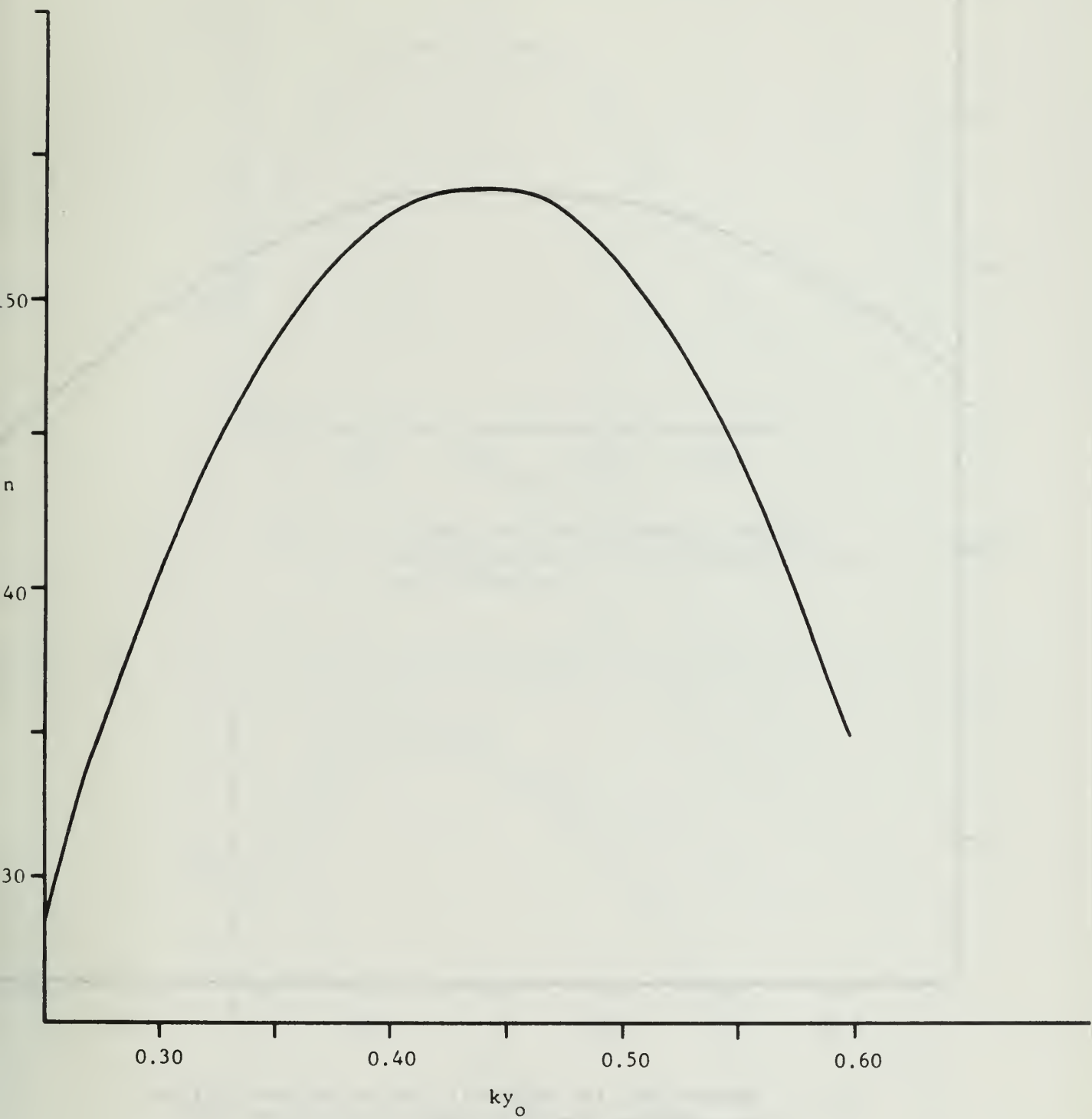


Fig. 8. Growth rate for hyperbolic tangent profile, $w = 4000$ km, $H = 50$ km, with friction.

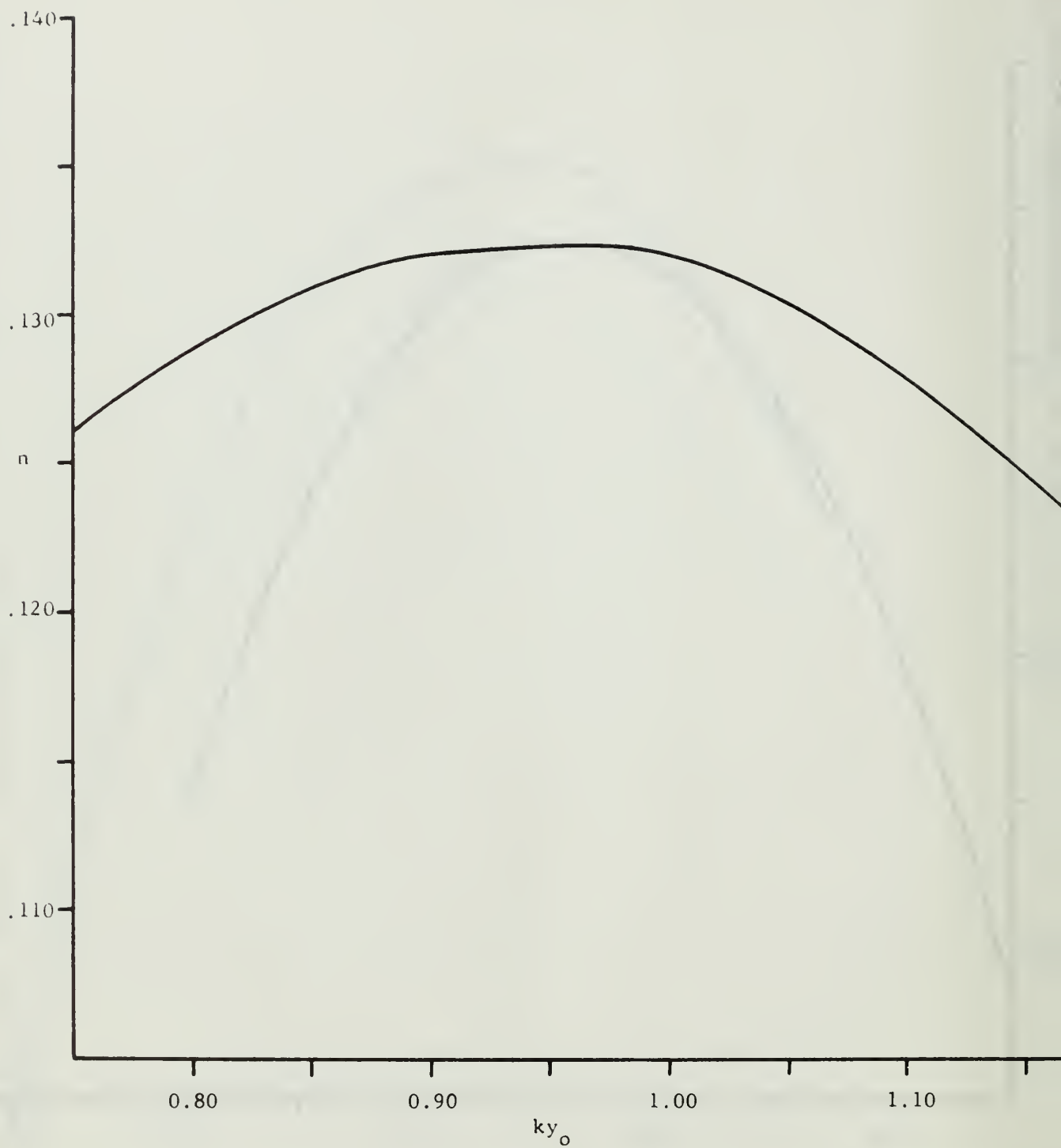


Fig. 9. Growth rate for hyperbolic secant squared profile, $w = 2000$ km, $H = 50$ km, with friction.

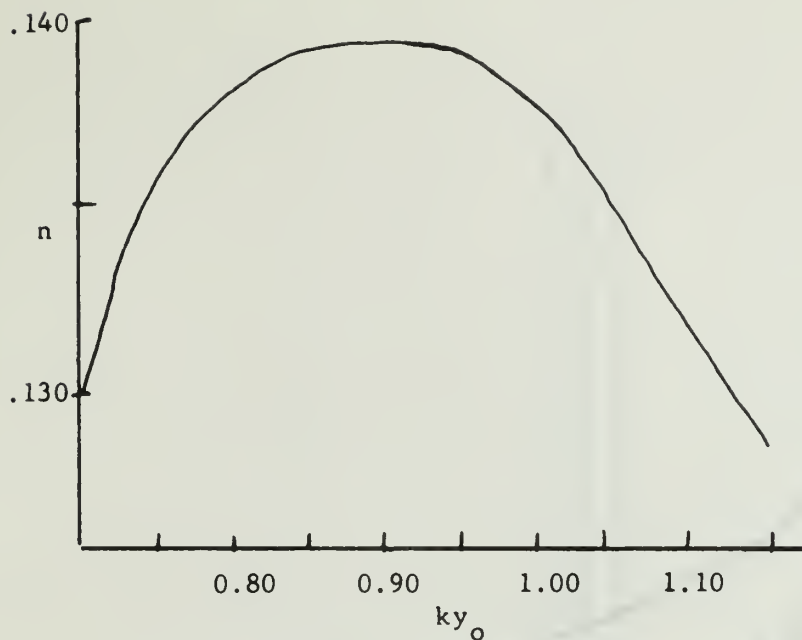


Fig. 10. Growth rate for hyperbolic secant squared profile, $w = 2000$ km, $H = 25$ km, with friction.

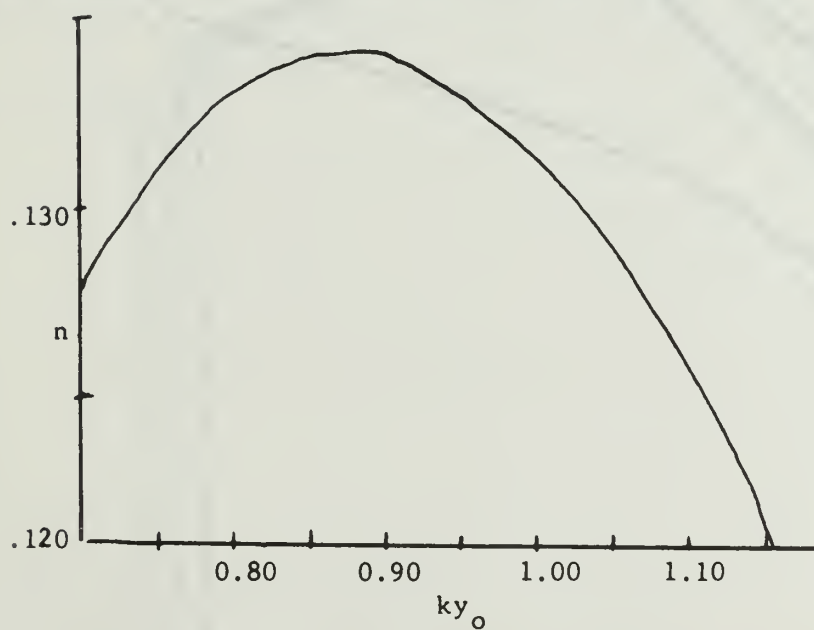


Fig. 11. Growth rate for hyperbolic secant squared profile, $w = 4000$ km, $H = 25$ km, with friction.

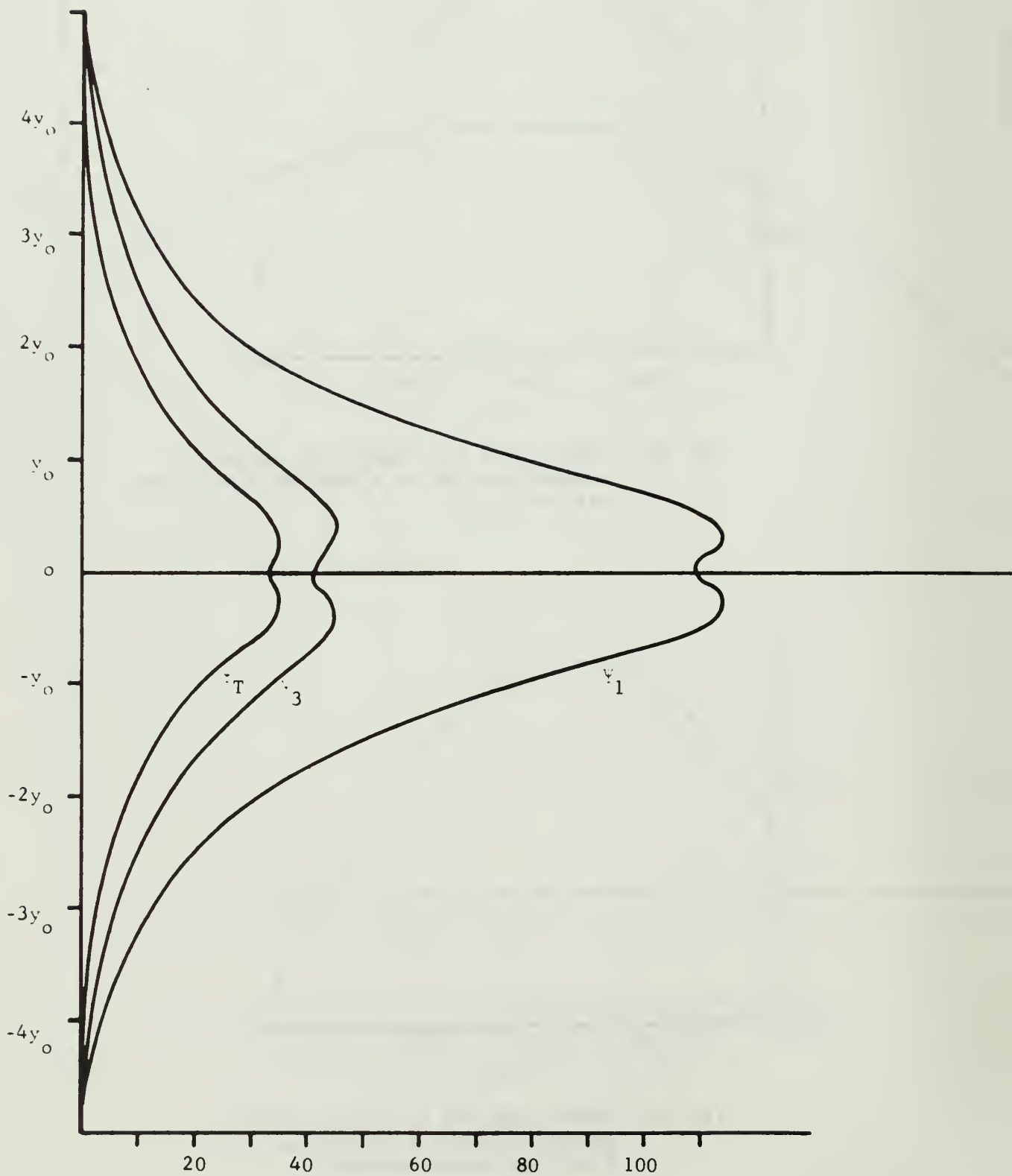


Fig. 12. Amplitudes of Ψ_T , Ψ_1 , and Ψ_3 for hyperbolic tangent profile plotted against arbitrary scale, $w = 4000$ km, $H = 50$ km, and wave number = 0.45.

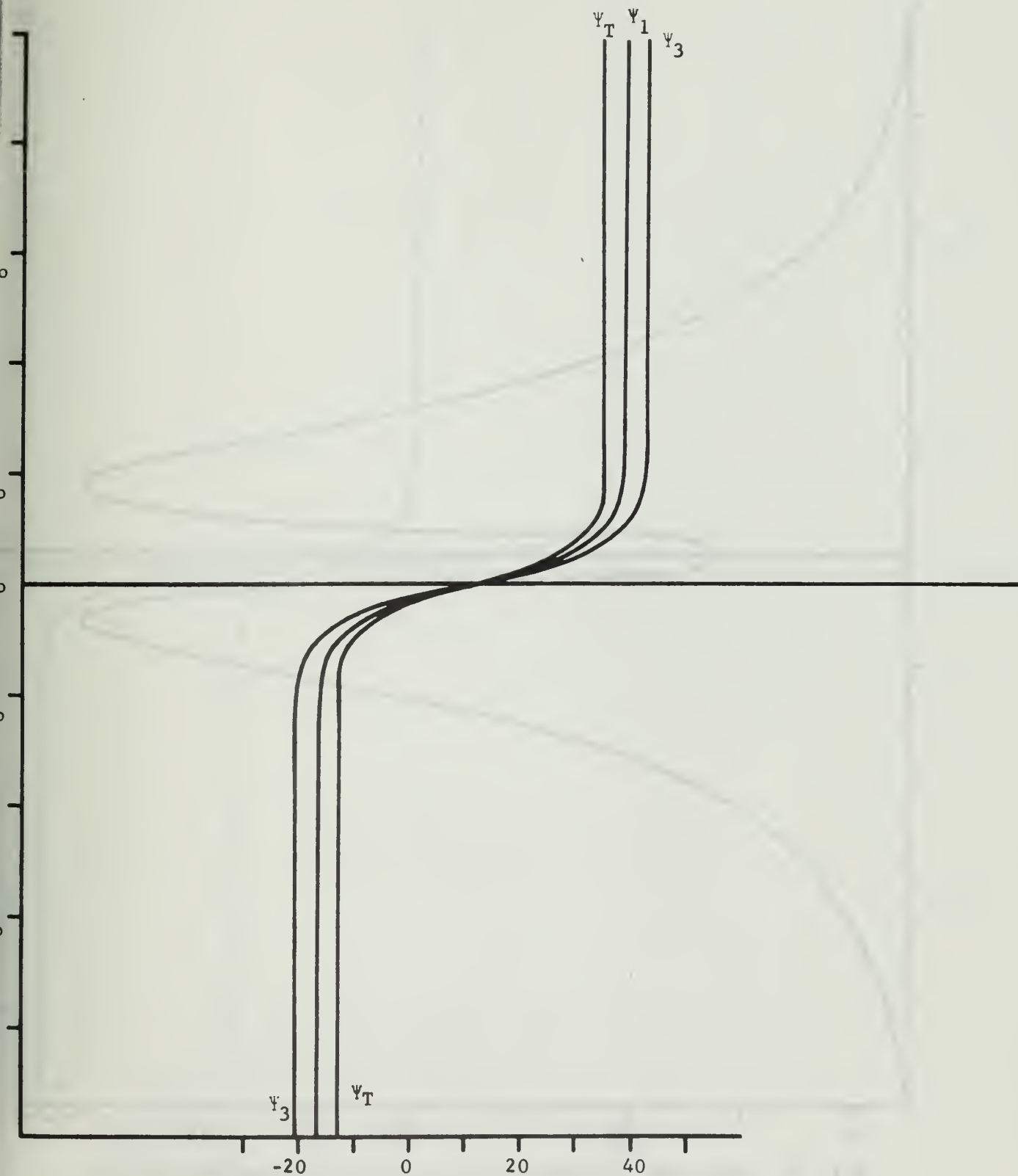


Fig. 13. Phase relationships corresponding to amplitudes of fig. 12.

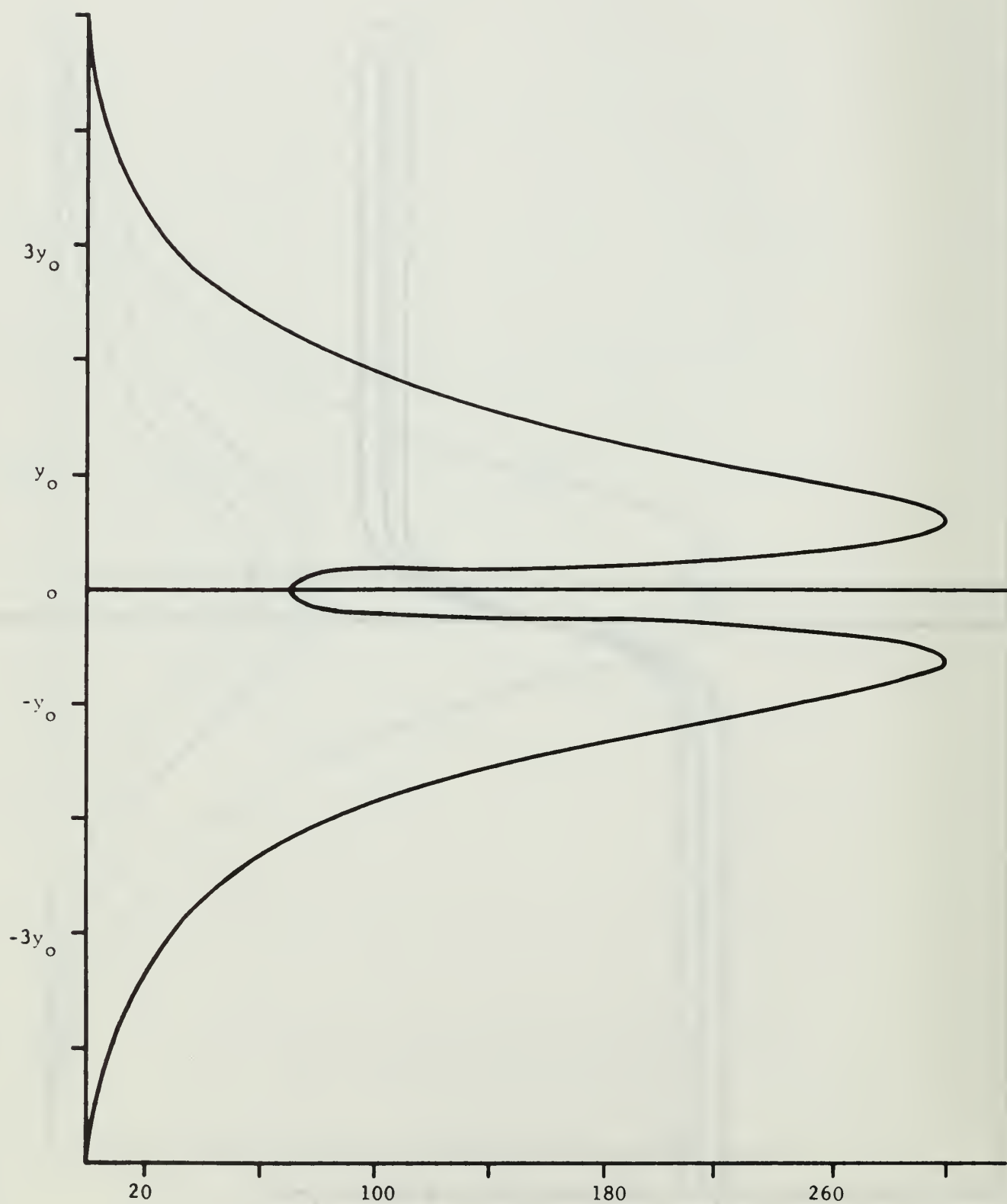


Fig. 14. Amplitude of omega, arbitrary scale for same case as figs. 12 and 13.

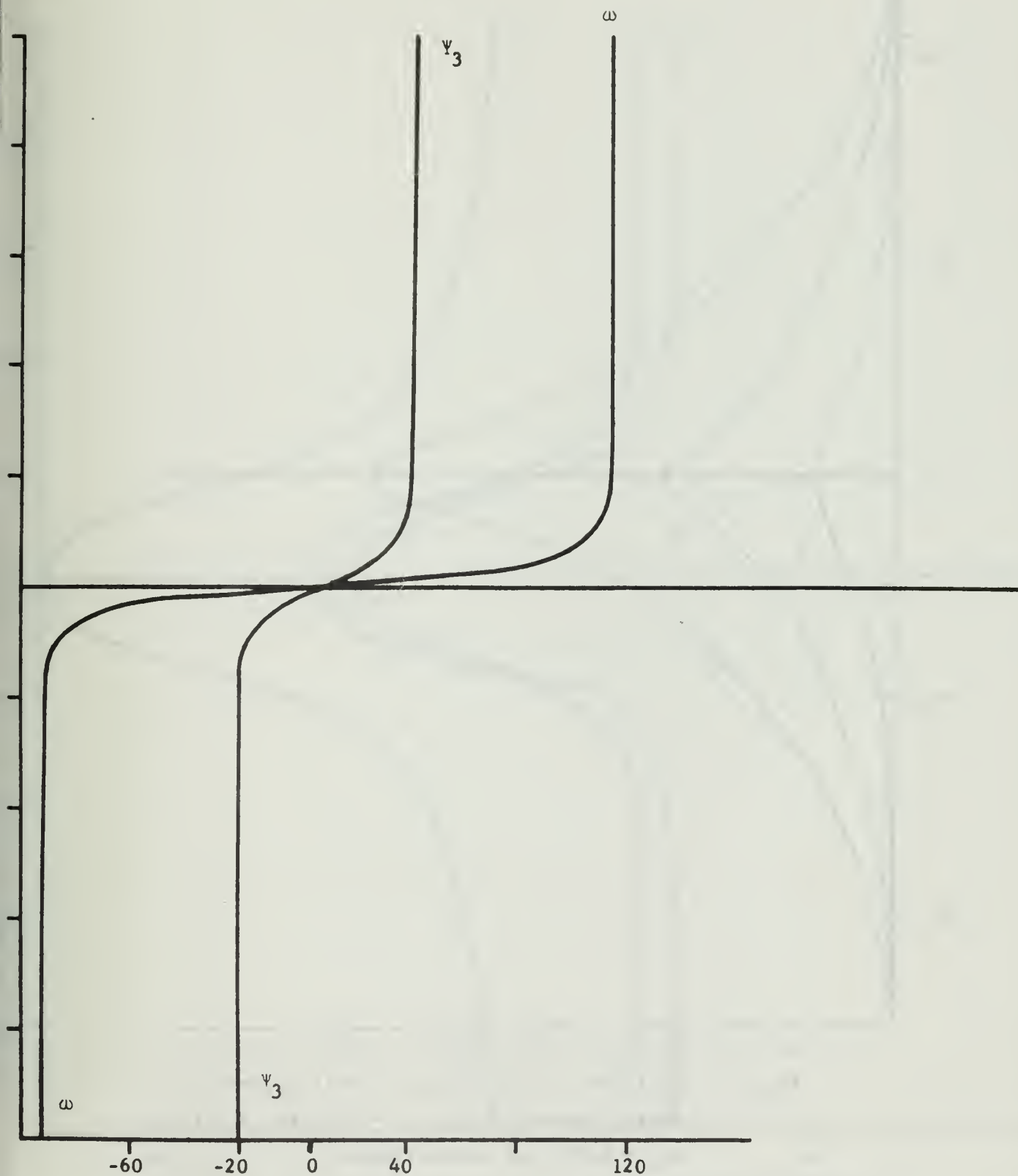


Fig. 15. Phase relationship between ψ_3 and ω , same conditions as figs. 12, 13, and 14.

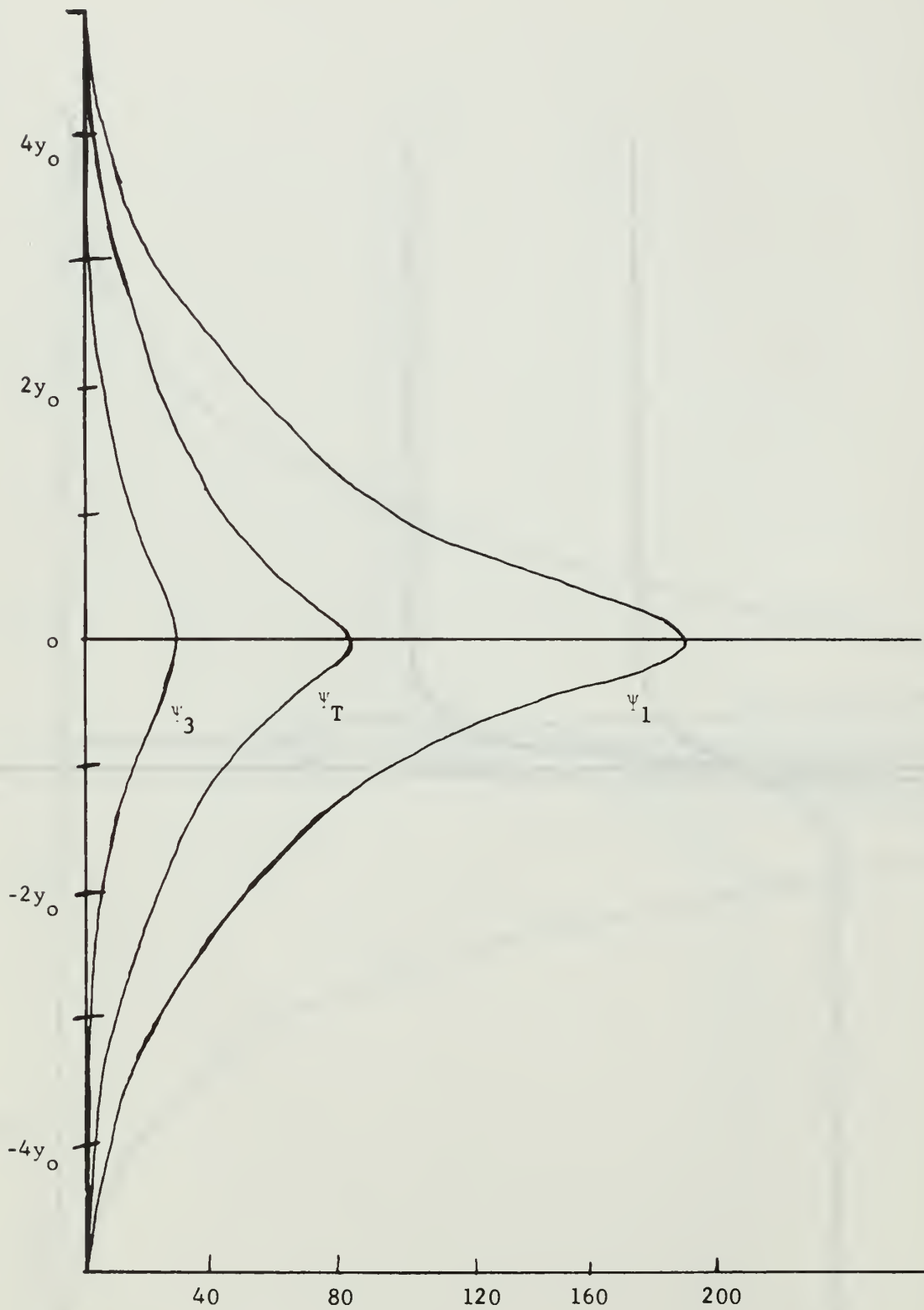


Fig. 16. Amplitude of Ψ_1 , Ψ_3 , and Ψ_T with hyperbolic secant squared profile, $w = 2000$ km, $H = 25$ km, $ky_0 = 0.95$, and scale arbitrary.

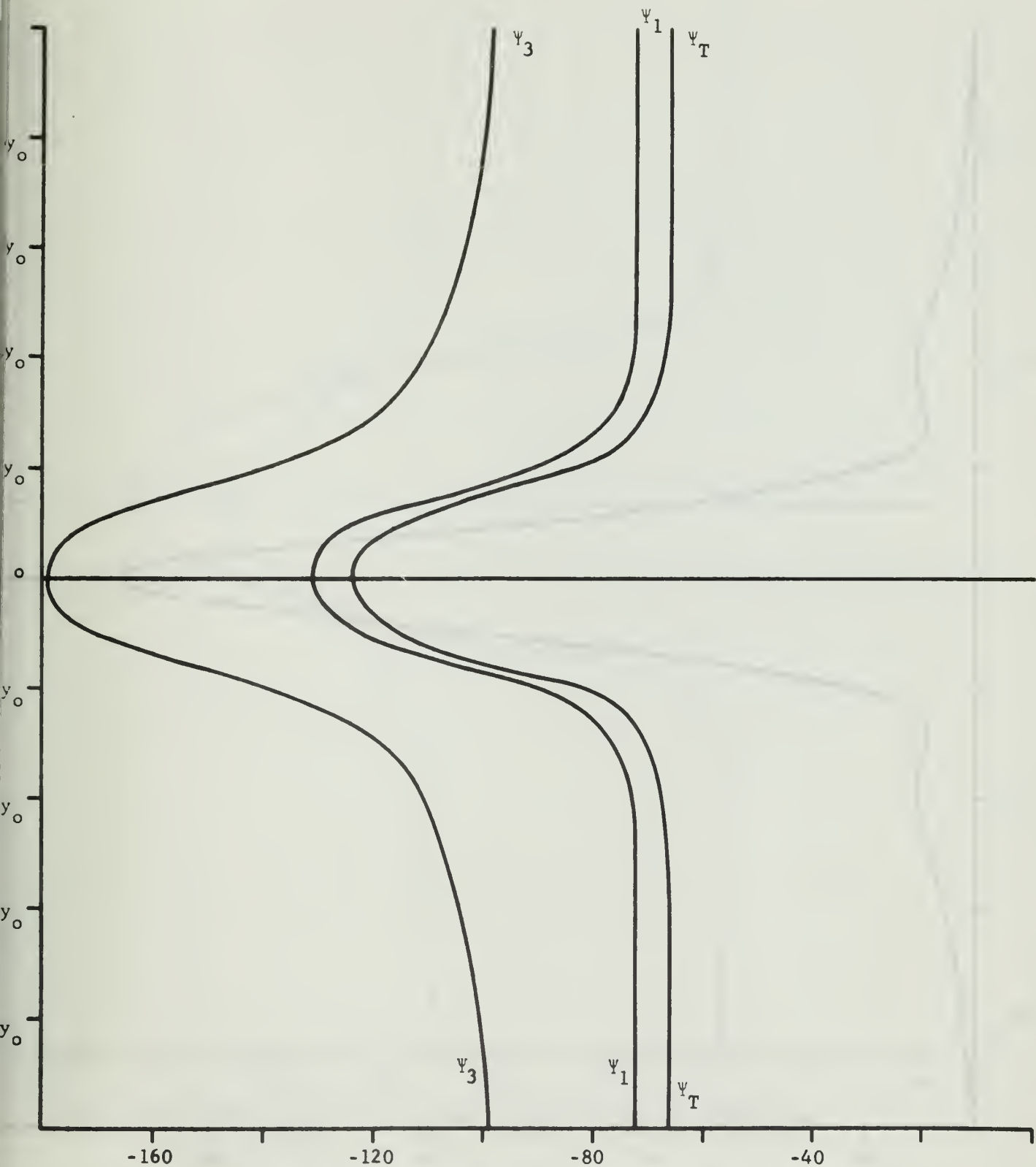


Fig. 17. Phase relationship for ψ_1 , ψ_3 , ψ_T for same conditions as fig. 16.

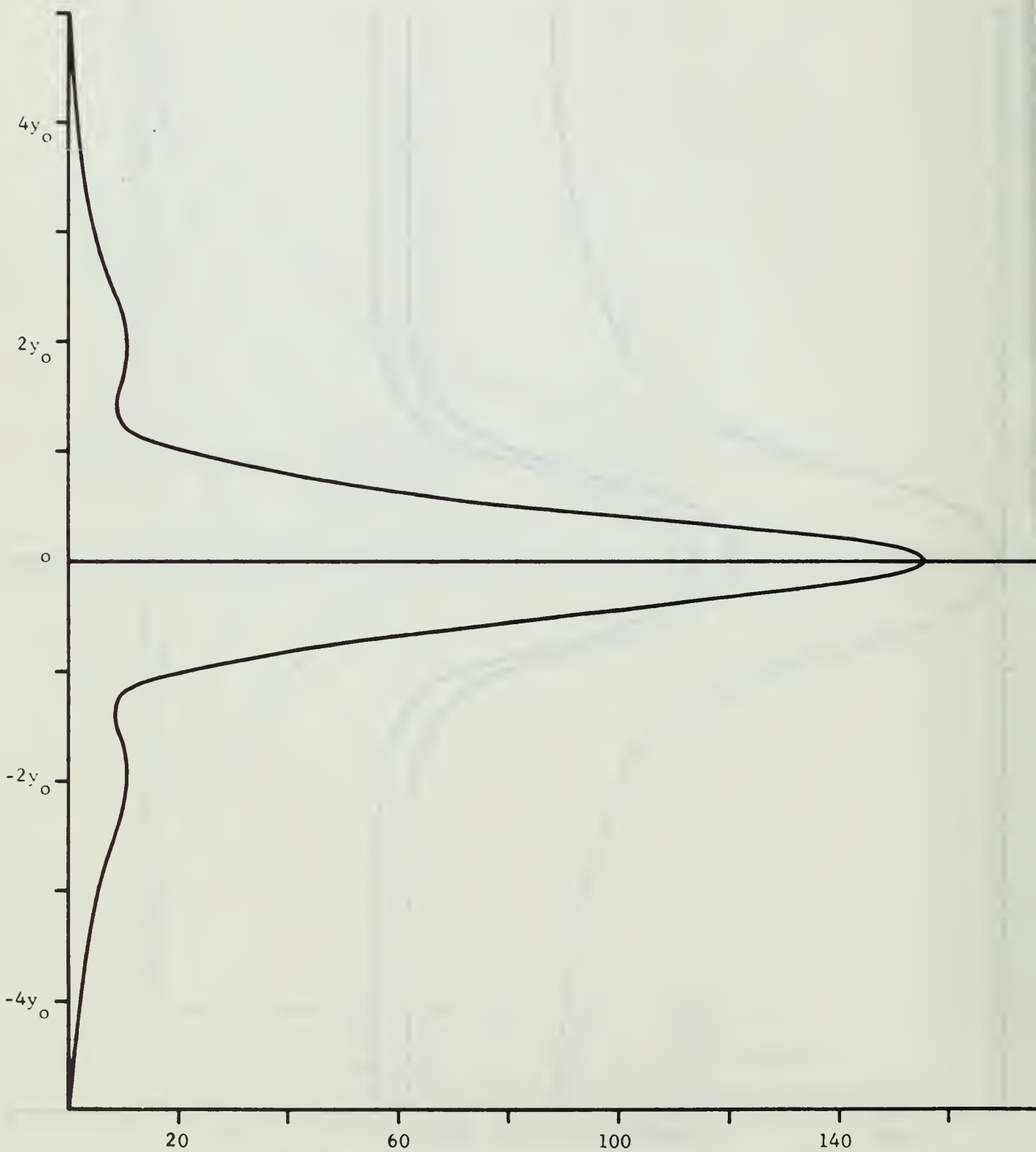


Fig. 18. Amplitude of omega, conditions as in fig. 16.

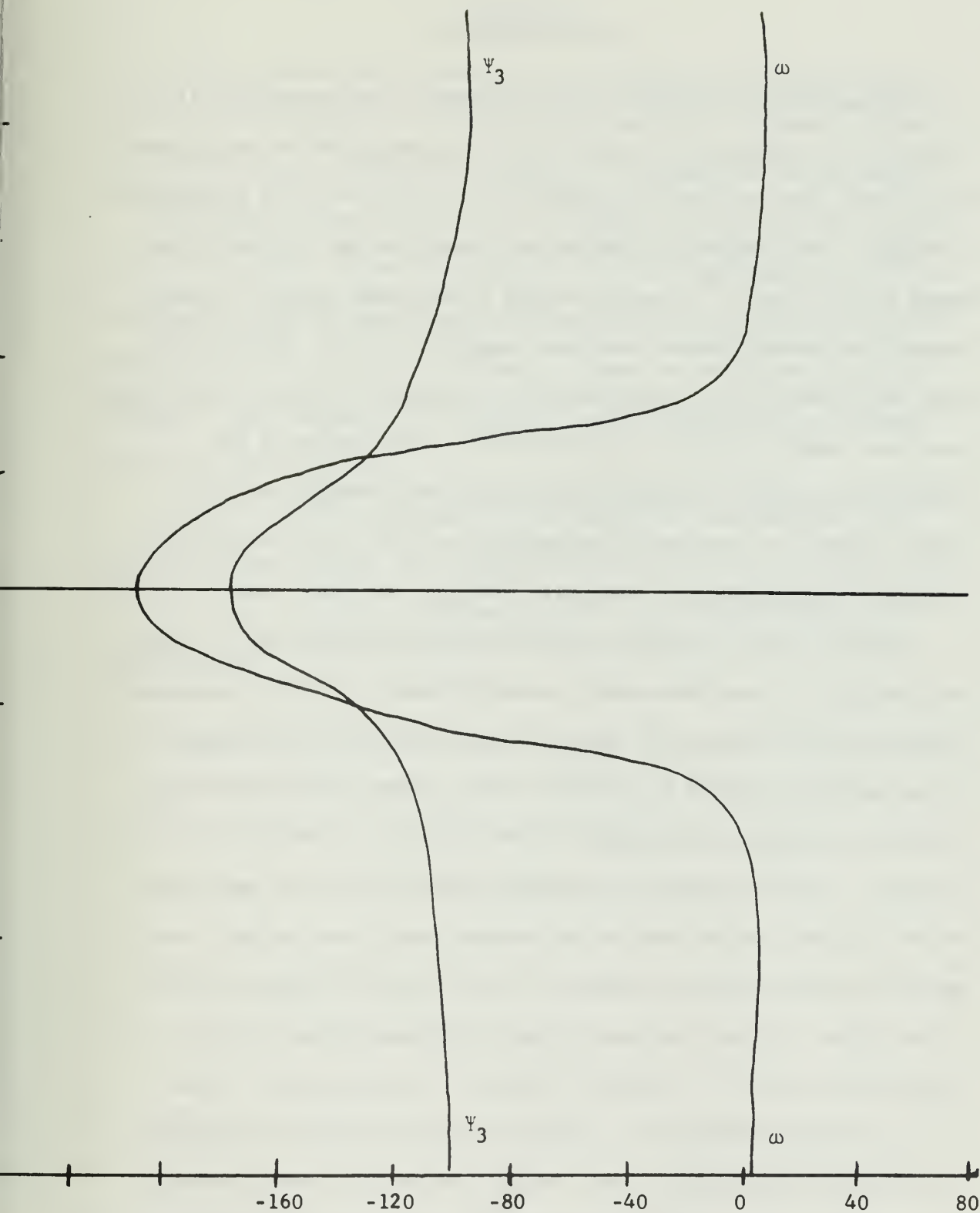


Fig. 19. Phase relationship between omega and Ψ_3 for conditions in fig. 16.

8. CONCLUSIONS

The easterly wave model developed appears to be reasonable if the assumption of barotropic instability as the energy source is accepted. Basic zonal flow has been introduced by two profiles, both independent of height. The temperature variations arose from the action of the Ekman friction terms. Waves developed by the model behaved in many respects as easterly waves have been observed to act. Results show that the growth rate of disturbances is a function of wave number, therefore wave length, as well as other factors. Separation of the boundaries to greater distances made some small changes but the greater effect is obtained by decreasing the grid size, which also required changing the time step size, through the shear zone.

Vertical motions produced by the hyperbolic tangent profile are very similar to those observed in easterly waves, in that the maximum sinking motion is upwind of the lower level ridge and the maximum rising motion is upwind of the lower level trough. The disturbance maintains its phase relationship in the vertical so that no tilt is observed. With the hyperbolic secant squared profile the amplitude of the vertical motion outside the maximum shear zone is small and again the rising motion is upwind of the trough and sinking upwind of the ridge. Within the area of large horizontal shear the convergent area moves to a position downwind of the low level trough. It is not known whether this is observationally verified along the Intertropical Convergence Zone. Using this profile, the hyperbolic secant squared, the model has developed a solution that indicates a definite eastward tilt with height. This tilt has been verified by observations. Perhaps some combination of the two profiles would be more realistic in depicting actual waves.

A more complete investigation of the effect of friction on the symmetric secant squared profile appears warranted. There is, also, a definite need to include the effects of condensation in the model.

Non-linear effects, their role in changing the mean wind profile and the structure of the disturbance, are very important and must be considered. Use of the primitive equations or the balance equations would seem to offer the most effective means of incorporating these effects. They appear to be crucial if an easterly wave is to grow into a tropical storm.

Always of utmost importance is the need for more detailed and extensive observations, but nowhere is this as true as of the tropics. No model can be developed and adequately tested without detailed observations.

REFERENCES

- Betchov, Robert, and William O. Criminale, Jr., 1967: Stability of Parallel Flows, Academic Press, New York.
- Charney, J. G., 1963: A note on large-scale motions in the tropics. Journal of the Atmospheric Sciences, Vol. 20, 607-609.
- Charney, J. G., 1969: A further note on large-scale motions in the tropics. Journal of the Atmospheric Sciences, Vol. 26, 182-185.
- Charney, J. G., and A. Eliassen, 1949: A numerical method for predicting the perturbations of the middle-latitude westerlies. Tellus, Vol. 1, 38-54.
- Charney, J. G., and A. Eliassen, 1964: On the growth of the hurricane depression. Journal of the Atmospheric Sciences, Vol. 21, 68-75.
- Garcia, R. V., 1956: Barotropic waves in straight parallel flow with curved velocity profiles. Tellus, Vol. 8, 82-93.
- Jacobs, Stanley J., and Aksel Wiin-Nielsen, 1966: On the stability of a barotropic basic flow in a stratified atmosphere. Journal of the Atmospheric Sciences, Vol. 23, 682-687.
- Kuo, H. L., 1949: Dynamic instability of two-dimensional non-divergent flow in a barotropic atmosphere. Journal of Meteorology, Vol. 6, 105-122.
- Palmer, C. E., 1951: Tropical meteorology. Compendium of Meteorology, American Meteorological Society, Boston, 859-880.
- Richtmyer, R. D., 1957: Difference Methods for Initial Value Problems, Interscience Publishers, Inc., New York.
- Riehl, H., 1954: Tropical Meteorology, McGraw-Hill Book Company, New York.
- Schminke, T. K., 1968: On the structure of easterly waves. M.S. Thesis, University of Utah, Salt Lake City.
- Thompson, P. D., 1961: Numerical Weather Analysis and Prediction, The MacMillan Company, New York.
- Yanai, Michio, and Tsuyoshi Nitta, 1967: Computation of vertical motion and vorticity budget in a Caribbean easterly wave. Journal of the Meteorological Society of Japan, Vol. 45, 444-466.
- Yanai, Michio, and Tsuyoshi Nitta, 1968a: Finite difference approximations for the barotropic instability problem. Journal of the Meteorological Society of Japan, Vol. 46, 389-403.

Yanai, Michio, and Tsuyoshi Nitta, 1968b: Barotropic instability of the equatorial easterly current. Paper presented at the International Symposium of Numerical Weather Prediction, Tokyo, Japan, 26 November-4 December 1968.

2.


```

8 FORMAT(1H0,23H FE OUTPUT FREQUENCY = ,F5.0,13H INTEGRATIONS)
7 WRITE(6,7)N,AA,TIME
7 FORMAT(1H0,16H GRID SIZE, N = ,I3,27H POINTS, AMPLITUDE, AA = ,F
16.2,21H TIME STEP SIZE = ,F10.2,9H SECONDS.)
C
C
C
C
CONSTANTS USED ARE
C
THIS SECTION DEFINES COMPUTED CONSTANTS USED THROUGHOUT PROGRAM
C
N IS THE NUMBER OF POINTS IN THE ONE DIMENSIONAL ARRAY.
C
ANNN IS THE NUMBER OF INTERVALS BETWEEN THE N POINTS.
C
WRITE(6,602) ANNN
602 FORMAT(4X,7HANNN = ,F7.2)
SIGMA = 0.000049879999
H = 25000.0
PNOT = 100.0
TOTAL DISTANCE FROM BOUNDARY TO BOUNDARY
M = FLOAT(N-1) * H
WRITE(6,955) M
955 FORMAT(1H0,42H TOTAL DISTANCE W BETWEEN THE N POINTS IS ,F12.2,8H
1 METERS.)
C
IN THE PROGRAM NOTATION DEL Y IS H
YZERO = 8.0 * H
RK IS AREAL VALUE OF K BUT IS THE NON-DIMENSIONAL WAVE NUMBER
NK = 11.0/(10.0 * YZERO)
NI = ((N-1) / 2) + 1
UNOT = 10.0
PLE = 3.1415926535
IDA = 86400
IDHR = 3600
ITIME = TIME
ANL = (2.0*PIE)/RK
WRITE(6,15) FNOT,BETA,SIGMA
15 FORMAT(1H0,5X,7HFNOT = ,F15.12,5X,7HBETA = ,F18.15,5X,8HSIGMA = ,F
15.12)
WRITE(6,13) ANL,H,PNOT
13 FORMAT(1H0,15H WAVELENGTH L = ,F10.0,40H METERS, DISTANCE BETWEEN
1 POINTS, H = ,F10.0,18H METERS, PNOT = ,F6.2,11H CENTIBARS.)
AKAY = 2.0*PIE / ANL
SOK = AKAY*AKAY
FNOTSQ = FNOT*FNOT
SQPNOT = PNOT * PNOT
SQMU = ( 8.0 * FNOTSQ ) / ( SQPNOT * SIGMA )
FSOK = FNOT*SOK
FSOMU = FNOT*SQMU
FUJ = AKAY / FNOT
TFUK = AKAY / 2.0*FNOT

```

```

C      PKMU = SQK + SOMU
C      SKMU = SQK - SOMU
C      RETAK = BETA*AKAY
C      HI = 1.0 / H
C      HSO = H * H
C      TH = 1.0 / (2.0*H)
C      SQH = 1.0 / (H*H)
C      TCUH = TH*SQH
C      WCONST = 4.0 / (PNOT * SIGMA)
C      ALPHA = PIE/M
C      FRICTION TERMS
C      AAA = 10.0
C      GRAVITY = 9.8
C      RCON = 287.0
C      ABSTMP = 300.0
C      CONSL = ((FNOT*GRAVITY)/(RCON*ABSTMP*2.0))* SQR( AAA/FNOT )
C      WRITE(6,16) CONSL
16  FORMAT(1H0,10H CONSL = ,E16.8)
C      ALLDANCE IS MADE FOR HEATING TERMS
C      ATEA = 2.0
C      DTEA = 0.0
C      HEATING ADDED DENOTED AS S
C      S = (SOMU*GRAVITY*DTEA*ATEA*SQR( AAA/FNOT ) )/(8.0*ABSTMP*FNOT)
C      WRITE(6,18) S
18  FORMAT(1H0,5H S = ,E16.8)

      INITIALIZE INDEXES

      THE FOLLOWING ARE COUNTERS FOR:
      END OF THE PROGRAM, WHERE NXT IS THE NUMBER OF INTEGRATIONS.
      NXT=0
C      PRINT OUT FREQUENCY
C      NXTPR = 1
C      PRINT OUT OF FE RELATIVE TO PRINT OUT FREQUENCY
C      FECNT=1.0
C      TEST2 IS FOR THE FIRST TIME STEP DATA SHIFT.
C      TEST2 = 1.0
C      TEST3 IS FOR RETURN FROM PRINTING ORIGINAL DATA.
C      TEST3 = 1.0

      BOUNDARY VALUES

      THESE VALUES NEVER CHANGE.  OPERATE FROM L TO M NOT 1 TO N
      THIS SECTION PUTS THE VALUE INTO ALL PRESENT TIME LOCATIONS
      LESS THE BOUNDARIES.

```

```

C
C      L=2
C      M=N-1
C
C      TO TEST THE EQUATIONS SET THE FOLLOWING VALUES,
C
      A = 0.0
      R = 0.0
      C = 0.0
      F = 0.0
      E = 0.0
      F = 0.0
C
C      OPERATING VALUES
C      1000  FORMAT(F15.12)
C            DO 101 I=1,N
C            READ(5,1000) A
C            ATDPR(I) = A
C            CONTINUE
C      101  DO 102 I=1,N
C            READ(5,1000) B
C            RTDPR(I) = B
C            CONTINUE
C      102  DO 103 I=1,N
C            CTDPR(I) = C
C            CONTINUE
C      103  DO 104 I=1,N
C            DTDPR(I) = D
C            CONTINUE
C      104  DO 105 I=1,N
C            Y = H * FLOAT(I-N)
C            E = -(FNOT*UNDT*YZERO) * TANH(Y/YZERO)
C            ETDPR(I) = E
C            CONTINUE
C      105  DO 106 I=1,N
C            FTDPR(I) = F
C            CONTINUE
C      106  FOR THE LOWER BOUNDARY VALUES
C            I=1
C            GO TO 24
C      25  FOR THE UPPER BOUNDARY
C            I=N
C      24  ATDPR(I) = 0.0
C            RTDPR(I) = 0.0
C            CTDPR(I) = 0.0
C            DTDPR(I) = 0.0
C            FTDPR(I) = 0.0
C            ASY(I) = 0.0

```



```

C FIRST TIME INTEGRATION
C THIS CUTS TIME STEP IN HALF FOR FIRST FORECAST TIME.
C
C      TIMAJ = TIME / 2.0
C      CALL FCST
C      NCOUNT = 1
C      GO TO 800
C
C      RESET TIME STEP FOR REMAINING OPERATIONS
C
C      803 TIMAJ = TIME
C          NXPRT = 1
C          TEST2 = 3.0
C
C      MAIN LOOP FOR FORECASTING
C
C      900 CONTINUE
C          CALL FCST
C          NCOUNT = NCOUNT + 1
C
C      THIS INSURES THAT COMPUTE OMEGA ONLY AT TIMES DESIRED
C
C      IF(NCOUNT.LT.336) GO TO 800
C      DO 10 I = 1, N
C      1 WCONST*(N-I+1) = WCONST * ((CTDF(N-I+1)-CTDPA(N-I+1))/(2.0*TIME) + FUK
C      2 * ((ESY(N-I+1) * BTDP(N-I+1)) - (ESY(N-I+1) * DTDPA(N-I+1))))
C      3 - WCONST*((S/SQMU)*(ADY(N-I+1)-CDY(N-I+1)) - SOK*(ATDPA(N-I+1)) -
C      4 CTDPA(N-I+1)))
C      1 WCONST*(N-I+1) = WCONST * ((DTDF(N-I+1) - DTDPA(N-I+1))/(2.0 * TIME) +
C      2 FUK*((ESY(N-I+1) * CTDPA(N-I+1)) - FSY(N-I+1) * ATDPA(N-I+1)))
C      3 - WCONST*((S/SQMU)*(RDY(N-I+1) - DDY(N-I+1)) - SOK*(BTDP(N-I+1)) -
C      4 DTDPA(N-I+1)))
C      10 CONTINUE
C
C      NOW SHIFT THE DATA, MOVING THE PRESENT DATA INTO THE
C      PAST ARRAY AND THE FUTURE DATA INTO THE PRESENT ARRAY.
C
C      800 NO 801 I = 1, N
C          ATDPA(I) = ATDPA(I)
C          ATDPA(I) = BTDP(I)
C          CTDPA(I) = CTDPA(I)
C          DTDPA(I) = DTDPA(I)
C          ETDPA(I) = ETDPA(I)
C          FTDPA(I) = FTDPA(I)
C      CONTINUE
C      801 DO 802 I = 1, N
C          ATDPA(I) = ATDPA(I)

```



```

      RTDPR(I) = BTDF(I)
      CTDPR(I) = CTDF(I)
      DTDPR(I) = DTDFF(I)
      FTDPR(I) = ETDFF(I)
      FTDPR(I) = FTDFF(I)
802 CONTINUE

C
C INCREMENT COUNTERS
C
      NXT = NXT + 1
      NXTPR = NXTPR + 1
C
C TEST FOR PRINTOUT
C
903 IF( NXTPR .GE. NPRT) GO TO 909
      IF ( TEST2 .LT. 2.0 ) GO TO 803
C
C TEST FOR END OF RUN
C
902 IF(NXT .LT. NRUN) GO TO 900
      WE HAVE REACHED THE MAX NUMBER OF INTEGRATIONS DESIRED, AND WE
      GO TO 901
C
C PRINT OUT OF DATA
C
      COMPUTE THE HEADINGS FOR THE OUTPUT.
C
909 IPUT = NXT * ITIME
      IDAY = IPUT / IDA
      IHRFT = IPUT - ( IDAY * IDA )
      ISEC = IHRFT - ( IHR * IHR )
      WRITE(6,910) NXT, IDAY, IHR, ISEC
910 FORMAT(1H, 19H INTEGRATION NUMBER, I4, 25H, A TOTAL LAPSED TIME
      1 OF, I4, 5H DAYS, I3, 7H HOURS, I4, 9H SECONDS.,/)
      WRITE(6,922)
922 FORMAT(126H 1 D A E B F C
      1 2 1./)
932 FORMAT(1H, I3, 3X, E16.8, 3X, E16.8, 3X, E16.8, 3X, E16.8, 3X, E16.
      28, 3X, I3)
      DO 930 I = 1, N
      IK = N - I + 1
      WRITE(6,932) IK, ATDPR(N-I+1), RTDPR(N-I+1), CTDPR(N-I+1),
      * DTDPR(N-I+1), ETDPR(N-I+1), FTDPR(N-I+1), IK
930 CONTINUE

```

```

C
C
C      NOW CALCULATE THE ENERGY RELATIONSHIPS OF THE MODEL
C
C      CALL ENERGY
C      FECNT = FECNT + 1.0
C      FEPRT IS RELATIVE TO THE NUMBER OF TIMES PRINTOUT OCCURS
C      IF (FECNT .LT. FEPRT ) GO TO 911
C      WRITE(6,222)
222  FORMAT(1H0,15H I AMPLITUDE OF A AND B, PHASE,A,B AMPLITUDE
C      ZE OF C AND D, PHASE2,C,D WAMP PHASE3,WC,WS )
C
C      COMPUTE PHASE ANGLE IN DEGREES
C
WAMP = 0.0
CAMP1 = 0.0
CAMP2 = 0.0
PHASE = 0.0
PHASE2 = 0.0
PHASE3 = 0.0
PHASE4 = 0.0
PHASE5 = 0.0
FEAMP = 0.0
FEAMP2 = 0.0
NASSUM = 0
C
C      FAKE IS USED TO PREVENT DIVISION BY ZERO ON THE BOUNDARIES
C
FAKE = 0.1E-19
DO 220 I=1,N
  IJ = N-I+1
  IF ( I .EQ. 1 ) GO TO 292
  IF ( I .EQ. N ) GO TO 292
  ESY(I) IS CALCULATED IN ENERGY AND DOES NOT HAVE TO BE REPEATED.
  WC = ((FSY(N-I+1) * BTDPR(N-I+1)) - (ESY(N-I+1) * DTDP(N-I+1))) / (2.0 * TIME) + FUK
  2 * ((FSY(N-I+1) * BTDPR(N-I+1)) - (ESY(N-I+1) * DTDP(N-I+1)))
  3 - WCONST * ((S/SOMU) * ((ADY(N-I+1) - CDY(N-I+1)) - SOK * (ATDPA(N-I+1) -
  4 CTDPR(N-I+1))))
  WS = WCONST * ((DTDF(N-I+1) - DTDP(N-I+1)) / (2.0 * TIME) +
  2 FUK * ((ESY(N-I+1) * CTDPR(N-I+1)) - FSY(N-I+1) * ATDPR(N-I+1)))
  3 - WCONST * ((S/SOMU) * ((BDY(N-I+1) - DDY(N-I+1)) - SOK * (BTDP(N-I+1) -
  4 DTPA(N-I+1))))
  IF (ABS(WC) .GT. 0.0) GO TO 298
  IF (ABS(WS) .GT. 0.0) GO TO 298
  299 PHASE3 = ATAN(WS/FAKE)
  NASSUM = NASSUM + 1
  GO TO 297
298 PHASE3 = ATAN(WS/WC)
297 IF ((ABS(PHASE3) - 0.8) .GT. 0.0) GO TO 170
WAMP = WC / COS ( PHASE3 )

```


[illegible]

```

911 IF( TEST3.LT. 2.0 ) GO TO 950
    IF( TEST2.LT. 2.0 ) GO TO 803
    NXPRT = 0
C
C    TO TEST FOR THE END OF THE PROGRAM WE
C
C    GO TO 902
C
C    CONTINUE
C
C    PHASE4 IS FEE1 CASE, A+C, B+D
C    PHASE5 IS FEE3 CASE, A-C, B-C
C
C    WRITE(6,258)
258 FORMAT(1H1,73H 1  AMPLITUDE FEE1      PHASE FEE1      AMPLITUDE
*FEE3
    NASSUM = 0.0
    DO 257 I=1,N
    IJ = N-I+1
    FEE8 = ATDPR(N-I+1) - CTDPR(N-I+1)
    FEE9 = BTDPR(N-I+1) - OTDPR(N-I+1)
    IF(ABS(FEE8).GT.0.0) GO TO 398
    PHASE5 = ATAN(FEE9/FAKE)
    NASSUM = NASSUM + 1
399 GO TO 397
    PHASE5 = ATAN( FEE9 / FEE8 )
398 IF( ABS( PHASE5 ) - 0.8 ) .GT. 0.0 ) GO TO 329
397 FEAMP2 = FEE8 / COS( PHASE5 )
    GO TO 325
329 FEAMP2 = FEE9 / SIN( PHASE5 )
325 PHASE5 = 57.29578 * PHASE5
    IF( FEAMP2 .GE. 0.0 ) GO TO 355
    IF( PHASE5 .GT. 0.0 ) GO TO 345
    PHASE5 = PHASE5 + 180.0
    GO TO 348
345 PHASE5 = PHASE5 - 180.0
348 FEAMP2 = -FEAMP2
355 FEE6 = ATDPR(N-I+1) + CTDPR(N-I+1)
    FEE7 = BTDPR(N-I+1) + OTDPR(N-I+1)
    IF(ABS(FEE6).GT.0.0) GO TO 395
    PHASE4 = ATAN(FEE7/FAKE)
    NASSUM = NASSUM + 1
    GO TO 394
395 PHASE4 = ATAN( FEE7 / FEE6 )
394 IF( ABS( PHASE4 ) - 0.8 ) .GT. 0.0 ) GO TO 229
    FEAMP = FEE6 / COS( PHASE4 )
    GO TO 225
229 FEAMP = FEE7 / SIN( PHASE4 )

```



```

C
DO 302 I=1,N
  AEO(N-I+1) = WCONST*((CTDF(N-I+1)-CTDPA(N-I+1))/(2.0*TIME) + FUK
2*((FSY(N-I+1) * BTDP(N-I+1))-(ESY(N-I+1) * DTDPR(N-I+1)))
3-WCONST*((S/SOMU)*((ADV(N-I+1)-CDY(N-I+1))-SOK*(ATDPA(N-I+1))-
4CTDPR(N-I+1)))
  REQ(N-I+1) = WCONST*((DTDF(N-I+1)- DTDPA(N-I+1))/(2.0 * TIME) +
2FUK*((ESY(N-I+1)* CTDPR(N-I+1)) -FSY(N-I+1) * ATDPR(N-I+1)))
3-WCONST*((S/SOMU)*((BDY(N-I+1)-DDY(N-I+1))-SOK*(BTDPA(N-I+1))-
4DTDPA(N-I+1)))
302 CONTINUE
  WRITE(6,312)
312 FORMAT(1H1,20H OMEGA = MC + WS)
  CALL MAP
C
FEM AND FET REVISITED
FE M WITH A,B
C
DO 303 I=1,N
  AEO(I) = ATDPR(I)
  REQ(I) = BTDP(I)
303 CONTINUE
  WRITE(6,313)
313 FORMAT(1H1,20H FE M WITH A,B )
  CALL MAP
DO 304 I=1,N
  AEO(I) = CTDPR(I)
  REQ(I) = DTDPR(I)
304 CONTINUE
  WRITE(6,314)
314 FORMAT(1H1,20H FE T WITH C,D )
  CALL MAP
  NEWMAN = NEWMAN + 1
  IF(NEWMAN.LT.2) GO TO 2
  GO TO 3
2 BETA = 2.29E-11
  WRITE(6,5)
5 FORMAT(2X,36H* * BETA IS REAL FOR ALL THE REST)
  GO TO 9
3 CALL GETIME (IET)
  XX = IET * 0.000026
  WRITE(6,1) XX
1 FORMAT(3X,17HTIME FOR RUN IS ,E16.6,7HSECONDS)
  STOP
END

```

۱۱۱۱۱

۱۱۱۱


```

C      ESY(I)=(ETDPR(I+1)-ETDPR(I-1))*TH
C      FSY(I)=(FTDPR(I+1)-FTDPR(I-1))*TH
C
C      SUM OF THE ENERGY CALCULATIONS
C
C      SASY = SASY + ASY(I) * ASY(I)
C      SBSY = SBSY + BSY(I) * BSY(I)
C      SCSY = SCSY + CSY(I) * CSY(I)
C      SDSY = SDSY + DSY(I) * DSY(I)
C      SESY = SESY + ESY(I) * ESY(I)
C      SFSY = SFSY + FSY(I) * FSY(I)
C
C      ADJUST THE SUMS FOR THE ENERGY EQUATIONS
C
C      SA = SA + ATDPR(I) * ATDPR(I)
C      SB = SB + BTDPR(I) * BTDPR(I)
C      SC = SC + CTDPR(I) * CTDPR(I)
C      SD = SD + DTDPR(I) * DTDPR(I)
C      SE = SE + ETDPR(I) * ETDPR(I)
C      SF = SF + FTDPR(I) * FTDPR(I)
C
C      800 CONTINUE
C
C      USING A ONE SIDED DIFFERENCE SCHEME ALONG THE BOUNDARIES
C
C      I = L
C      GO TO 810
C
C      809 I = N
C      810
C      ASY(I) = ( ASY(I) - ASY(I-1) ) * * HI
C      BSY(I) = ( BSY(I) - BSY(I-1) ) * * HI
C      CSY(I) = ( CSY(I) - CSY(I-1) ) * * HI
C      DSY(I) = ( DSY(I) - DSY(I-1) ) * * HI
C      ESY(I) = ( ESY(I) - ESY(I-1) ) * * HI
C      FSY(I) = ( FSY(I) - FSY(I-1) ) * * HI
C
C      COMPLETION OF THE SUMS
C
C      SASY = SASY + (.5 * ASY(I) * ASY(I) )
C      SBSY = SBSY + (.5 * BSY(I) * BSY(I) )
C      SCSY = SCSY + (.5 * CSY(I) * CSY(I) )
C      SDSY = SDSY + (.5 * DSY(I) * DSY(I) )
C      SESY = SESY + (.5 * ESY(I) * ESY(I) )
C      SFSY = SFSY + (.5 * FSY(I) * FSY(I) )
C
C      IF ( I .EQ. L ) GO TO 809
C
C      COLLECT ENERGY
C      DISTURBANCE KINETIC ENERGY OR DKE
C
C      DKE=(0.25 *(SOK*(SA + SB + SC + SD ) + ( SASY + SBSY + SCSY +

```

```

1 SDSY ) ) / ANNN
C DISTURBANCE POTENTIAL ENERGY OR DPE
C DPE =(SQMU * 0.25 * (SC + SD) ) / ANNN
C MEAN FLOW KINETIC ENERGY OR ENMKE
C ENMKE = ( 0.5 * ( SESY + SFSY ) ) / ANNN
C MEAN FLOW POTENTIAL ENERGY OR ENMPE
C ENMPE = ( SQMU * 0.5 * SF ) / ANNN
C TOTAL ENERGY IS
C
C ENED = DKE + DPE
C ENEM = ENMKE + ENMPE
C TOTEM = ENED + ENEM
C WRITE(6,24) DKE,DPE,ENMKE,ENMPE
C 24 FORMAT(1H0,6H DKE =,E16.8,7H, DPE =,E16.8,9H, ENMKE =,E16.8,9H, EN
C 2 MPPE =,E16.8)
C 20 FORMAT(1H0,22H DISTURBANCE ENERGY =,E16.8,20H MEAN FLOW ENERGY = ,
C *E16.8,19H TOTAL ENERGY IS =,E16.8)
C RETURN
C END

```

```

C SUBROUTINE RCHMYR(XEQ,XTDPR,XTDPA,XTDF)
C CALCULATES EXACT SOLUTION FOR THE DATA FIELD
C
C DIMENSION ATDPA(100), BTDPA(100), CTDPA(100), DTDPA(100), ETDPA(100),
C *FTDPA(100), ATDPR(100), BTDPR(100), CTDPR(100), DTDPR(100), ETDPR(100),
C *FTDPR(100), AEQ(100), BEQ(100), CEQ(100), DEQ(100), EEQ(100), FEEQ(100),
C *ASY(100), BSY(100), CSY(100), DSY(100), ESY(100), FSY(100), ADV(100),
C DIMENSION BDY(100), CDY(100), DDY(100), EDY(100), FDY(100), ATY(100),
C *RTY(100), CTY(100), DTY(100), ETY(100), VDY(100), VE(100),
C *VF(100), DVX(100), XEQ(100), XTDPA(100), XTDPR(100), XTDPR(100),
C COMMON N,L,M,H,HI,TH,TCUH,HSQ,SQH,$QK,SQMU,FSDK,FSQMU,FUK,TFUK,
C 2 BETAK PKMU,$KMU,TIME,TIMAJ,ANNN,VB,SA,$B,SC,SD,SE,SF,NXT,RK,PIE
C 3 CONSI
C 2 ATDPA, BTDPA, CTDPA, DTDPA, ETDPA, FTDPA, BTDPA,
C 2 ATDPR, BTDPR, CTDPR, DTDPR, ETDPR, FTDPR,

```



```

3      ATDF ,BTDF ,CTDF ,DTDF ,ETDF ,FTDF
4AEQ,BEQ,CEQ,DEQ,EEO,FEQ,ASY,BSY,CSY,DSY,ESY,FSY,
5 ADY,BDY,CDOY,DDY,EDY,FDY,ATY,BTY,CTY,DTY,ETY,FTY

      BOUNDARY CONDITIONS

C      VD(1) = 0.0
C      VD(N) = 0.0
C      VE(1) = 0.0
C      VE(N) = 0.0
C      VF(1) = 0.0
C      VF(N) = 0.0
C      DVX(1) = 0.0
C      DVX(N) = 0.0

C      RICHMYER SOLUTION
C      CALCULATE COEFFICIENTS FOR NEXT STEP
C
C      DO 450 I=L,M
C      VD(I) = -2.0*HSQ*TIMAJ*XEQ(I)
C      VE(I) = 1.0 / ( VB - VE(I-1) )
C      VF(I) = ( VD(I) + VF(I-1) ) * VE(I)
C      CONTINUE
C      CALCULATES VALUES FOR EACH POINT.
C      DO 454 I = 1,M
C      DVX(M-I+1) = (VE(M-I+1) * DVX(M-I+2)) + VF(M-I+1)
C      CONTINUE
C      RCHMYR TECHNIQUES ENDS HERE.  NEXT WE PUT VALUES INTO THE FUTURE ARRAY
C      DO 458 I=1,N
C      XTDF(I) = XTDP(A(I) + DVX(I))
C      CONTINUE
C      RETURN
C      END

```

```

SUBROUTINE MAP
  DIMENSION ATDPA(100), BTDPA(100), CTDPA(100), DTDPA(100), ETDPA(100),
  * FTDPA(100), ATDPR(100), BTDPR(100), CTDPR(100), DTDPR(100), ETDPR(100),
  * FTDPR(100), ATDF(100), BTDF(100), CTDF(100), DTD(100), ETD(100),
  * ASD(100), BSY(100), CSY(100), DSY(100), ESY(100), FSY(100),
  * ADY(100),
  DIMENSION BDY(100), CDY(100), DDY(100), EDY(100), FDY(100),
  * RTY(100), CTY(100), DTY(100), ETY(100), FTY(100),
  COMMON N, L, M, H, HI, TH, TCUH, HSO, SQH, SQK, SQMU, FSQMU, FUK, TFUK,
  2 BETAK, PKMU, SKMU, TIME, TIMAJ, ANNN, VB, SA, SB, SC, SD, SE, SF, NXT, RK, PIE,
  3 CONS1, S
  COMMON ATDPA, BTDPA, CTDPA, DTDPA, ETDPA, FTDPA, BTDPA,
  2 ATDPR, BTDPR, CTDPR, DTDPR, ETDPR, FTDPR,
  3 ATDF, BTDF, CTDF, DTD, ETD, FTD,
  4 AEQ, BEQ, CEQ, DEQ, EEQ, FEQ, ASY, BSY, CSY, DSY, ESY, FSY,
  5 ADY, BDY, CDY, DDY, EDY, FDY, ATY, BTY, CTY, DTY, ETY, FTY
  DO 301 I = 1, N
  DO 302 J = 1, 11
  RKX = (PIE/10.0) * FLOAT ( J-1 )
  ASY(J) = (AEQ(N-I+1) * COS(RKX) + BEQ(N-I+1) * SIN(RKX)) * 0.2 + ETD
  * PR(N-I+1)
302 CONTINUE
  IJ = N-I+1
  WRITE(6,304)IJ,(ASY(J),J=1,11),IJ
304 FORMAT(1H,13,11(E11.3),3X,13,/)
301 CONTINUE
  WRITE(6,320)
320 FORMAT(1H1)
  DO 311 I = 1, N
  DO 312 J = 1, 21
  PKX = (PIE/10.0) * FLOAT ( J-1 )
  ASY(J) = (AEQ(N-I+1) * COS(RKX) + BEQ(N-I+1) * SIN(RKX)) * 0.2 + ETD
  * PR(N-I+1)
312 CONTINUE
  IJ = N-I+1
  WRITE(6,314)IJ,(ASY(J),J=1,21),IJ
314 FORMAT(1H,13,11(E11.3),3X,13,/)
311 CONTINUE
  RETURN
END

```

```

C
C
C
SUBROUTINE FCST
C
C CALCULATES NEW VALUES BY FINITE DIFFERENCE AND CALLS RCHMYR.
C
DIMENSION ATDPA(100), BTDPA(100), CTDPA(100), DTDPA(100), ETDPA(100),
*FTDPA(100), ATDF(100), BTDF(100), CTDF(100), DTDf(100), ETDf(100),
*FTDf(100), AEO(100), BEO(100), CEO(100), DEO(100), EEO(100), FEO(100),
*ASY(100), BSY(100), CSY(100), DSY(100), ESY(100), FSY(100), ADY(100),
DIMENSION BDY(100), CDY(100), DDY(100), EDY(100), FDY(100), ATY(100),
*BTY(100), CTY(100), DTY(100), ETY(100), GLOB(800)
COMMON N, L, M, H, I, TH, TCUH, HSO, SQH, SQK, SOMU, FSQK, FSQMU, FUK, TFUK,
2 BETAK, PKMU, SKMU, TIME, TIMAJ, ANNN, VB, SA, SB, SC, SD, SE, SF, NEXT, RK, PIE,
3 CONSI, S
COMMON ATDPA, CTDPA, DTDPA, ETDPA, FTDPA, BTDPA,
2 COMMON ATDPR, BTDPR, CTDPR, DTDPR, ETDPR, FTDPR,
3 ATDF, BTDF, CTDF, DTDf, ETDf, FTDf,
4 AEO, BEO, CEO, DEO, EEO, FEO, ASY, BSY, CSY, DSY, ESY, FSY,
5 ADY, BDY, CDY, DDY, EDY, FDY, ATY, BTY, CTY, DTY, ETY, FTY,
GLOB(1) = 0.0
GLOB(N) = 0.0
GLOB(N+1) = 0.0
GLOB(N+N) = 0.0
C
C
C FRICTION TERMS
C
DO 120 I=L,M
GLOB(I) = { ADY(I)-CDY(I) } -SQK * { ATDPA(I) - CTDPA(I) }
GLOB(I+N) = (BDY(I)-DDY(I) ) - SQK*(BTDPA(I)-DTDPA(I) )
120 CONTINUE
DO 500 I=L,M
C
C
C SINGLE DERIVATIVES FOR A POINT
C
ASY(I)=(ATDPR(I+1)-ATDPR(I-1))*TH
BSY(I)=(BTDPR(I+1)-BTDPR(I-1))*TH
CSY(I)=(CTDPR(I+1)-CTDPR(I-1))*TH
DSY(I)=(DTDPR(I+1)-DTDPR(I-1))*TH
ESY(I)=(ETDPR(I+1)-ETDPR(I-1))*TH
FSY(I)=(FTDPR(I+1)-FTDPR(I-1))*TH
C
C DOUBLE DERIVATIVES FOR A POINT
C
ADY(I) = (ATDPR(I+1) + ATDPR(I-1) - 2.0 * ATDPR(I)) * SQH
BDY(I) = (BTDPR(I+1) + BTDPR(I-1) - 2.0 * BTDPR(I)) * SQH
CDY(I) = (CTDPR(I+1) + CTDPR(I-1) - 2.0 * CTDPR(I)) * SQH
DDY(I) = (DTDPR(I+1) + DTDPR(I-1) - 2.0 * DTDPR(I)) * SQH
EDY(I) = (ETDPR(I+1) + ETDPR(I-1) - 2.0 * ETDPR(I)) * SQH

```



```

      REQ(I) = FUK*((SOK*((ESY(I)*ATDPR(I)))+(FSY(I)*CTDPR(I))))
1 - (ESY(I)*ADY(I)) + (ETY(I)*ATDPR(I)) - (FSY(I)*COY(I)) +
2 - (ETY(I)*CTDPR(I)) + BETAK*ATDPR(I)
      CEQ(I) = FUK*((SOK*((-FSY(I)*BTDPRI(I)) - (ESY(I)*DTDPRI(I)*PKMU)
1 + (FSY(I)*RTDPR(I)*SQMU)+(ESY(I)*DDY(I))-(ETY(I)*BTDPRI(I))
2 + (FSY(I)*BDY(I)) - (ETY(I)*DTDPRI(I)) - BETAK*DTDPRI(I)
9 + (CONSI - S) * GLOB(I+N))
      DEQ(I) = FUK*((SOK*((FSY(I)*ATDPR(I)) + (ESY(I)*PKMU*CTDPR(I))
1 - (ESY(I)*COY(I)) + (ETY(I)*ATDPR(I)) - (SQMU*FSY(I)*ATDPR(I))
2 - (FSY(I)*ADY(I)) + (ETY(I)*CTDPR(I)) + BETAK*CTDPR(I)
9 + (CONSI - S) * GLOB(I+N))
      FEQ(I) = FUK*((ATDPR(I)*BDY(I)) - (BTDPRI(I)*ADY(I))
1 + (CTDPR(I)*DDY(I)) - (DTDPRI(I)*COY(I)))
      FEO(I) = FUK*((ATDPR(I)*(DDY(I)-DTDPRI(I)*PKMU)) - (BTDPRI(I)*
1 (COY(I)-CTDPR(I)*PKMU)) + (CTDPR(I)*(BDY(I)-BTDPRI(I)*SQK))
2 -(DTDPRI(I)*ADY(I)) - ATDPR(I)*SQK))
510 CONTINUE
      TIME DERIVATIVE STEP FOR A,B,C,D,E,F
      CALL THE RICHTMYER SOLUTION
      FOR AEO AND BEQ, VB DOES NOT CHANGE
      VR = 2.0 + HSQ * SQK
      CALL RCHMYR(AEQ,ATDPR,ATDPA,ATDFF)
      CALL RCHMYR(BEQ,BTDPRI,BTDPRI,DTDF)
      FOR CEO AND DEQ, VB DOES NOT CHANGE
      VB = 2.0 + HSQ*PKMU
      CALL RCHMYR(CEQ,CTDPR,CTDPA,CTDFF)
      CALL RCHMYR(DEQ,DTDPRI,DTDPA,DTDF)
      FOR EEO, VB IS
      VB = 2.0
      FOR FEQ, VR IS
      VR = 2.0 + HSQ*SQMU
      RETURN
      END

```


INITIAL DISTRIBUTION LIST

	<u>NO. OF COPIES</u>
1. Library Naval Postgraduate School Monterey, California 93940	2
2. Defense Documentation Center Cameron Station Alexandria, Virginia 22314	20
3. Naval Weather Service Command Washington Navy Yard Washington, D. C. 20390	1
4. Officer in Charge Naval Weather Research Facility Naval Air Station, Building R-48 Norfolk, Virginia 23511	1
5. Commanding Officer U. S. Fleet Weather Central COMNAVMARIANAS, Box 12 FPO San Francisco, California 96630	1
6. Commanding Officer Fleet Weather Facility P. O. Box 85 Naval Air Station Jacksonville, Florida 32212	1
7. Commanding Officer U. S. Fleet Weather Facility Box 72 FPO New York, New York 09510	1
8. Commanding Officer Fleet Numerical Weather Central Naval Postgraduate School Monterey, California 93940	1
9. Commanding Officer U. S. Fleet Weather Central Box 110 FPO San Francisco, California 96610	1
10. Commanding Officer U. S. Fleet Weather Central Box 31 FPO New York, New York 09540	1

	<u>NO. OF COPIES</u>
11. Commanding Officer U. S. Fleet Weather Facility, Box 30 FPO San Francisco, California 96652	1
12. AFCRL - Research Library L. G. Hanscom Field Attn: Nancy Davis/Stop 29 Bedford, Massachusetts 01730	1
13. Director, Naval Research Laboratory Attn: Tech. Services Info. Officer Washington, D. C. 20390	1
14. Department of Meteorology Code 51 Naval Postgraduate School Monterey, California 93940	3
15. Department of Oceanography Code 58 Naval Postgraduate School Monterey, California 93940	1
16. American Meteorological Society 45 Beacon Street Boston, Massachusetts 02128	1
17. Office of Naval Research Department of the Navy Washington, D. C. 20360	1
18. Commander, Air Weather Service Military Airlift Command U. S. Air Force Scott Air Force Base, Illinois 62226	2
19. Atmospheric Sciences Library Environmental Science Service Administration Silver Spring, Maryland 20910	1
20. Professor Victor Starr Department of Meteorology M.I.T. Cambridge, Massachusetts 03139	1
21. Dr. J. Pedlosky Department of Geophysical Sciences University of Chicago Chicago, Illinois 60637	1

NO. OF COPIES

- | | | |
|-----|--|---|
| 22. | Dr. Joanne Simpson
Experimental Meteorology Branch
Environmental Science Services Administration
Coral Gables, Florida 33124 | 1 |
| 23. | Dr. V. Jurcec
United Nations Development Program
Box 982
Cairo, United Arab Republic | 1 |
| 24. | Dr. G. C. Asnani
Observatory
Poona 5, India | 1 |
| 25. | National Center for Atmospheric Research
Box 1470
Boulder, Colorado 80302 | 1 |
| 26. | Dr. T. N. Krishnamurti
Department of Meteorology
Florida State University
Tallahassee, Florida 32306 | 1 |
| 27. | Dr. Fred Shuman
Director
National Meteorological Center
Environmental Science Services Administration
Suitland, Maryland 20390 | 1 |
| 28. | Dr. J. Smagorinsky
Director
Geophysical Fluid Dynamics Laboratory
Princeton University
Princeton, New Jersey 08540 | 1 |
| 29. | Professor N. A. Phillips
54-1422
M.I.T.
Cambridge, Massachusetts 02139 | 1 |
| 30. | Professor J. G. Charney
54-1424
M.I.T.
Cambridge, Massachusetts 02139 | 1 |
| 31. | Dr. F. Sanders
Department of Meteorology
M.I.T.
Cambridge, Massachusetts 02139 | 1 |

NO. OF COPIES

32.	Professor K. Ooyama Department of Meteorology New York University University Heights New York, New York 10453	1
33.	Dr. C. E. Palmer Institute of Geophysics UCLA Los Angeles, California 90024	1
34.	Dr. M. G. Wurtele Department of Meteorology UCLA Los Angeles, California 90024	1
35.	Dr. A. Arakawa Department of Meteorology UCLA Los Angeles, California 90024	1
36.	Captain Thomas Kent Schminke 2107 Randal Drive Bellevue, Nebraska 68005	1
37.	Dr. Herbert Riehl Department of Atmospheric Sciences Colorado State University Fort Collins, Colorado 80521	1
38.	Dr. Roger Terry Williams Department of Meteorology Naval Postgraduate School Monterey, California 93940	10
39.	Commander R. L. Newman Fleet Weather Facility Box 72 FPO New York, New York 09501	5

lassified

Security Classification

DOCUMENT CONTROL DATA - R & D

(Security classification of title, body of abstract and indexing annotation must be entered when the overall report is classified)

ORIGINATING ACTIVITY (Corporate author)		2a. REPORT SECURITY CLASSIFICATION	
Naval Postgraduate School Monterey, California 93940		Unclassified	
2b. GROUP			
REPORT TITLE			
A THEORETICAL INVESTIGATION OF THE STRUCTURE OF EASTERLY WAVES			
DESCRIPTIVE NOTES (Type of report and, inclusive dates)			
Masters Thesis, April, 1969			
AUTHOR(S) (First name, middle initial, last name)			
Robert L. Newman			
REPORT DATE	7a. TOTAL NO. OF PAGES	7b. NO. OF REFS	
April 1969	66	16	
CONTRACT OR GRANT NO.	9a. ORIGINATOR'S REPORT NUMBER(S)		
PROJECT NO.	N/A		
N/A	9b. OTHER REPORT NO(S) (Any other numbers that may be assigned this report)		
DISTRIBUTION STATEMENT			
This document has been approved for public release and sale; its distribution is unlimited.			
SUPPLEMENTARY NOTES		12. SPONSORING MILITARY ACTIVITY	
N/A		Naval Postgraduate School	
ABSTRACT			
<p>A simple two-level numerical model using the quasi-geostrophic forecast equations is developed. Equations are linearized and friction is introduced in the surface layer. Solutions are obtained numerically by using the initial value approach. Two wind profiles, $U = -U_0 \tanh y/y_0$ and $U = U_0 \operatorname{sech}^2 y/y_0$, are used and these are known to be unstable. For each wind profile the growth rate is determined as a function of the wave number. Some observed features of easterly waves are reproduced in the numerical solutions.</p>			

14

KEY WORDS

LINK A

LINK B

LINK C

ROLE

WT

ROLE

WT

ROLE

V

Barotropic instability

Two-level model

Wind profiles

Easterly wave

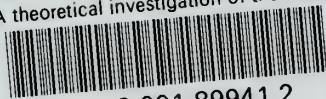
Growth rates

Phase relationships



thesN464

A theoretical investigation of the struc



3 2768 001 89941 2

DUDLEY KNOX LIBRARY